



NMRF/VR/03/2024



VERIFICATION REPORT

**NCUM Global Model Verification:
Pre-monsoon (MAM) 2024**

K. Niranjan Kumar, Sukhwinder Kaur, Mohana S. Thota, M. Venkatarami Reddy, Harvir Singh, Sushant Kumar, Anumeha Dube, and Raghavendra Ashrit

2024

**National Centre for Medium-Range Weather Forecasting
Ministry of Earth Sciences, Government of India
A-50, Sector-62, NOIDA-201 309, INDIA**

NCUM Global Model Verification: Pre-monsoon (MAM) 2024

K. Niranjan Kumar, Sukhwinder Kaur, Mohana S. Thota, M. Venkatarami Reddy, Harvir Singh, Sushant Kumar, Anumeha Dube, and Raghavendra Ashrit

NMRF/VR/03/2024

**National Centre for Medium-Range Weather Forecasting
Ministry of Earth Sciences, Government of India
A-50, Sector 62, NOIDA-201309, INDIA
www.ncmrwf.gov.in**

Data Control Sheet

1	Name of the Institute	National Center for Medium-Range Weather Forecasting
2	Document Number	NMRF/VR/03/2024
3	Date of Publication	July 2024
4	Title of the document	NCUM Global Model Verification: Pre-monsoon (MAM) 2024
5	Type of the document	Verification Report
6	Number of pages, figures, and Tables	45 pages, 32 figures, 4 Tables
7	Authors	K. Niranjana Kumar, Sukhwinder Kaur, Mohana S. Thota, M. Venkatarami Reddy, Harvir Singh, Sushant Kumar, Anumeha Dube, and Raghavendra Ashrit
8	Originating Unit	National Centre for Medium-Range Weather Forecasting (NCMRWF), A-50, Sector-62, NOIDA201 309, India.
9	Abstract	This report provides a comprehensive assessment of the NCMRWF's NCUM global model analysis and forecast performance during the Pre-monsoon season (MAM) of 2024. Aimed at both forecasters and model developers, the verification results are presented with a focus on biases in forecasted winds, temperature, humidity, and rainfall. These crucial insights enable forecasters to effectively interpret the model guidance, aiding in accurate and informed weather forecasting. The findings also offer valuable feedback to model developers, supporting continuous improvement efforts to enhance the model's forecasting capabilities.
10	References	17
11	Security classification	Unrestricted
12	Distribution	General

Table of Contents

S.No		P.No.
	Abstract	1
1.	Introduction	2
2.	NCMRWF Unified Modelling System & Verification datasets	3
	<i>2.1. Model Description</i>	3
	<i>2.2. Observed/analysis Data used for the verification</i>	3
3.	NCUM-G Analysis Mean and Anomalies during MAM 2024	4
	<i>3.1. Winds at 850, 700, 500, and 200 hPa levels</i>	4
	<i>3.2. Temperature at 850, 700, 500, and 200 hPa levels</i>	6
	<i>3.3. Relative Humidity at 850, 700, and 500 hPa levels</i>	8
4.	Systematic Errors in NCUM-G Forecasts	10
	<i>4.1. Winds at 850, 700, 500, and 200 hPa levels</i>	10
	<i>4.2. Temperature & Relative Humidity</i>	14
	<i>4.3. Surface (10m) winds</i>	20
	<i>4.4. Temperature at 2m</i>	21
	<i>4.5. Total Precipitable Water (PWAT)</i>	22
5.	Forecast Verification during MAM 2024	23
	<i>5.1. Rainfall Mean and Mean Error</i>	24
	<i>5.2. Categorical Scores of Rainfall Forecasts</i>	24
	<i>5.3. Categorical Scores of Tmax at 2m</i>	24
6.	Significant Weather during MAM 2024	27
	<i>6.1. Bay of Bengal SCS 'REMAL' during 24-28 May 2024</i>	27
	<i>6.1.1. Forecast Tracks and Strike Probability</i>	28
	<i>6.1.2. Forecast Track Errors</i>	29
	<i>6.1.3. Forecast Intensity Errors (Central Pressure and Max Sustained Wind)</i>	31
	<i>6.1.4. Forecast Landfall Error</i>	32
	<i>6.1.5. Verification of Strike Probability</i>	33
	<i>6.1.6. CRA Verification of Rainfall forecasts</i>	34
	<i>6.2. Western Disturbance & Heat Waves</i>	36
	<i>6.2.1. Western disturbances</i>	36
	<i>6.2.2. Heat Waves</i>	38
	<i>6.2.3. Observed and forecasted daily Tmax time series</i>	40
7.	Summary	42
8.	References	45

NCUM Global Model Verification: Pre-monsoon (MAM) 2024

**K. Niranjan Kumar, Sukhwinder Kaur, Mohana S. Thota, M. Venkatarami Reddy, Harvir Singh,
Sushant Kumar, Anumeha Dube, and Raghavendra Ashrit**

सारांश

यह रिपोर्ट 2024 के प्री-मॉनसून सीज़न (मार्च से मई) के दौरान रा.म.अ.मौ.पू.के. के एन.सी.यू.एम वैश्विक मॉडल विश्लेषण और पूर्वानुमान प्रदर्शन का व्यापक मूल्यांकन प्रदान करती है। पूर्वानुमानकर्ताओं और मॉडल डेवलपर्स दोनों के उद्देश्य से, सत्यापन परिणाम पूर्वानुमानित तापमान, आर्द्रता, वर्षा, और हवाओं में पूर्वाग्रहों पर ध्यान केंद्रित करके प्रस्तुत किए जाते हैं। ये महत्वपूर्ण अंतर्दृष्टि पूर्वानुमानकर्ताओं को मॉडल मार्गदर्शन की प्रभावी ढंग से व्याख्या करने में सक्षम बनाती हैं, जिससे सटीक और सूचित मौसम पूर्वानुमान में सहायता मिलती है। निष्कर्ष मॉडल डेवलपर्स को मूल्यवान प्रतिक्रिया भी प्रदान करते हैं, जो मॉडल की पूर्वानुमान क्षमताओं को बढ़ाने के लिए निरंतर सुधार प्रयासों का समर्थन करते हैं।

Abstract

This report provides a comprehensive assessment of the NCMRWF's NCUM global model analysis and forecast performance during the Pre-monsoon season (MAM) of 2024. Aimed at both forecasters and model developers, the verification results are presented with a focus on biases in forecasted winds, temperature, humidity, and rainfall. These crucial insights enable forecasters to effectively interpret the model guidance, aiding in accurate and informed weather forecasting. The findings also offer valuable feedback to model developers, supporting continuous improvement efforts to enhance the model's forecasting capabilities.

1. Introduction

This comprehensive report documents the performance evaluation of the global NCMRWF Unified Model (NCUM-G) forecasts during the Pre-monsoon season (MAM) of 2024. The primary objective of this assessment is to verify the accuracy and reliability of the forecasts by comparing them against model analyses and observations. The results are skillfully summarized, shedding light on the average biases and forecasting performances for the entire season. Given the diverse audience, the report is thoughtfully oriented towards forecasters and model developers, recognizing their distinct interests in understanding and improving the forecasting process. Sections 3 to 5 of the report examine the systematic biases found in the forecasted large-scale upper fields, encompassing crucial elements such as wind, temperature, humidity, and rainfall, among others. The insights provided in these sections prove to be invaluable in enabling forecasters to interpret the model forecasts more effectively and make informed decisions. Before the forecast evaluation, Section 2 sets the foundation by presenting a comprehensive description of the NCUM-G model, including details about the advanced data assimilation system employed at NCMRWF. Moreover, this section offers insights into the observational datasets utilized in this study, ensuring transparency and providing the context for the subsequent analyses. In Section 3, a detailed examination of the seasonal mean analysis and respective anomalies is presented, providing a holistic view of the model's performance throughout the Pre-monsoon season. Subsequently, Section 4 investigates the model's systematic errors, followed by a thorough validation of forecasts in Section 5. One of the highlights of this report is covered in Section 6, where verification for significant weather events of MAM 2024 takes center stage. The verification process involves assessing the model's performance in predicting important extreme weather systems, including the Bay of Bengal (BoB) severe cyclonic storm (SCS) 'REMAL' during 24-28 May 2024, Western Disturbances, and Heat Wave episodes. This analysis proves crucial for gauging the model's capabilities in capturing extreme weather events, which are often of immense significance to various stakeholders. Finally, Section 7 briefly summarizes the key findings, strengths, and limitations of the NCMRWF model forecasts during this Pre-monsoon season. The summary offers valuable takeaways for both forecasters and model developers, aiding them in refining the forecasting process and enhancing the model's performance in subsequent seasons.

2. NCMRWF Unified Modelling System & Verification datasets

2.1. Model Description

NCMRWF started using the Unified Model (UM) Partnerships' seamless prediction system operationally since 2012, and this system was named NCUM. The NCUM global Numerical Weather Prediction (NWP) system (NCUM-G) became operational in 2012 with a grid resolution of 25 km (NCUM-G: V1) for medium-range weather prediction. This was upgraded to 17 km horizontal resolution (NCUM-G: V3) in 2015, 12 km (NCUM-G: V5) in 2018, and 12 km resolution with improved model physics in 2020 (NCUM-G: V6). The present version (NCUM-G: V7) of NCUM-G has a horizontal grid resolution of ~12 km with 70 vertical levels in the atmosphere reaching 80 km height. It uses an "ENDGame" dynamical core, which provides improved accuracy of the solution of primitive model equations and reduced damping. This helps in producing finer details in the simulations of synoptic features such as cyclones, fronts, troughs, and jet stream winds. ENDGame also increases variability in the tropics, which leads to an improved representation of tropical cyclones and other tropical phenomena. The model uses improved physics options of GA7.2 (Walters et al., 2017). An advanced Data Assimilation (DA) method of Hybrid 4-Dimensional Variational (4D-Var) is used for the creation of NCUM global analysis. The advantage of the Hybrid 4D-Var is that it uses a blended background error, a blend of "climatological" background error, and day-to-day varying flow-dependent background error (derived from the 22-member ensemble forecasts). The hybrid approach is scientifically attractive because it elegantly combines the benefits of ensemble data assimilation (flow-dependent co-variances) with the known benefits of 4D-Var within a single data assimilation system (Barker, 2011). Various in-situ and remote-sensing observations are being used in the NCUM global DA system. New and novel observations are added to the DA system through in-house R&D and collaborations. A brief description of the NCUM Hybrid 4D-Var DA system is given by Kumar et al. (2021, 2020, & 2018). The surface analysis preparation system (SURF) prepares the surface analysis of snow, SST, sea ice, soil moisture, etc., for the NCUM-G model (SURF system includes Extended Kalman Filter based Land Data Assimilation System, which is used for soil moisture analysis).

2.2. Observed/analysis Data used for the Verification

The seasonal mean analysis and anomalies are studied using the fifth-generation European Centre for Medium-Range Weather Forecasts (ECMWF) reanalysis product (ERA-5) Hersbach et al., (2020) climatology (1979-2018). The high-resolution (12km) NCUM-G analysis data is interpolated to ERA-5 grid resolution ($0.25^{\circ} \times 0.25^{\circ}$). For verification of the forecasts, the NCUM-G model analysis is used. All systematic errors are computed at a native grid resolution of 12km.

Detailed quantitative rainfall forecast verification is based on the India Meteorological Department (IMD)-NCMRWF daily high-resolution (0.25°) rainfall analysis (Mitra et al. 2009, 2013). The rainfall analysis objectively analyses India Meteorological Department (IMD) daily rain gauge observations onto a 0.25° grid using a successive corrections technique with the GPM Satellite rainfall providing the first guess estimates. The model forecasts are gridded to the 0.25° observed rainfall grids over Indian land regions for 92 days from 1st March 2024 to 31st May 2024. As noted by Mitra et al. (2009), the merged analysis at 0.25° grid resolution is appropriate for capturing the large-scale rain features associated with the monsoon. The merging of the IMD gauge data into GPM estimates not only corrects the mean biases in the satellite estimates but also improves the large-scale spatial patterns in the satellite field, which is affected by temporal sampling errors (Mitra et al. 2009). Verification of daily temperature forecasts is carried out against the IMD daily observed gridded ($0.5^{\circ} \times 0.5^{\circ}$) maximum (Tmax) and minimum (Tmin) temperature data (Srivastava et al. 2009).

3. NCUM-G Analysis Mean and Anomalies during MAM2024

3.1. Winds at 850, 700, 500, and 200 hPa levels

In this section, we evaluate the mean analysis fields and anomalies relative to climatology for the period of March-April-May (MAM) 2024, focusing on Winds, Temperature, and Relative Humidity across four standard atmospheric pressure levels: 850 hPa, 700 hPa, 500 hPa, and 200 hPa. Anomalies are calculated against the backdrop of the fifth-generation European Centre for Medium-Range Weather Forecasts (ECMWF) reanalysis product, ERA5, utilizing climatological data spanning from 1979 to 2018. Figures 1a-d illustrate the mean winds and anomalies at the 850 hPa and 700 hPa levels as derived from the NCUM-G analysis. At these altitudes, the seasonal mean analysis from the NCUM-G model depicts northwesterly winds, with wind speeds increasing with altitude, ranging between 5 to 10 m/s. Additionally, an anticyclone presence is noted over the southern peninsular region. This anticyclonic circulation is particularly evident at the 700 hPa level across the southern peninsular region in the NCUM-G model analysis. These anomalous wind conditions at 850 hPa and 700 hPa are depicted in Figures 1c-d. The analysis reveals contrasting wind anomalies across the Indian subcontinent, with weaker winds in the north and stronger winds in the south compared to the ERA5 climatology. Over the equatorial Indian Ocean, especially in the southern latitudes, the NCUM-G analysis shows weaker winds, leading to strong anomalous easterlies. Consequently, in North India, the wind magnitude is observed to be lower relative to the ERA5 climatology, attributed to persistent anomalous easterlies.

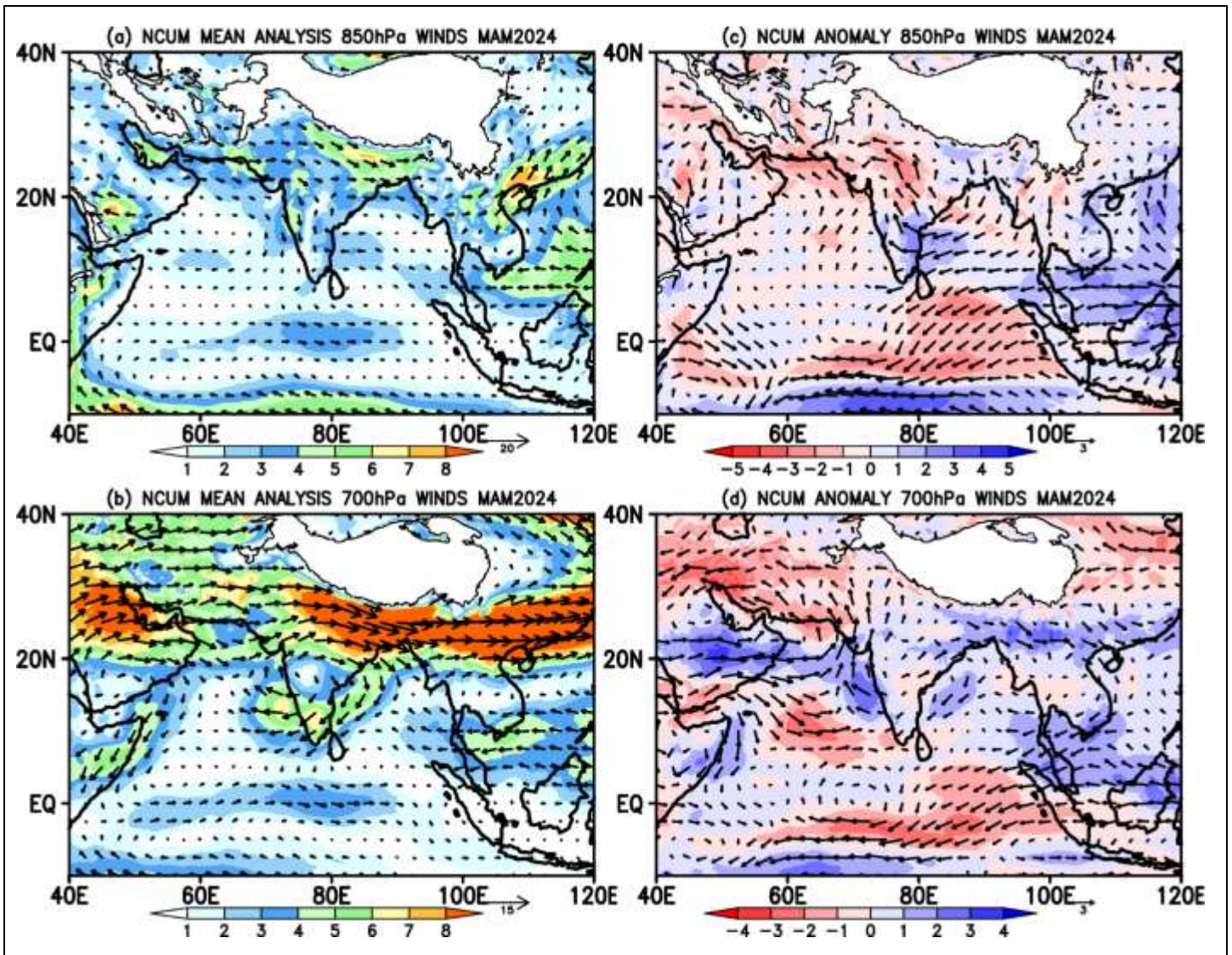


Figure 1. Mean winds at (a) 850 hPa and (b) 700 hPa in the NCUM-G Analysis during MAM 2024 (m/s). Right panels show the anomaly circulations at (c) 850 hPa and (d) 700 hPa.

The NCUM-G model analysis mean winds at the 500 hPa and 200 hPa levels, which correspond to the mid and upper troposphere, is shown in Figures 2a and 2b. As altitude increases, the mean wind speeds in the northern Indian region significantly intensify, rising from approximately 18 m/s to over 40 m/s in the upper troposphere. Conversely, wind speeds in the southern Indian region at these altitudes are notably weaker. Figures 2c and 2d illustrate the anomalous winds associated with the model analysis relative to the ERA5 climatology. Throughout the mid and upper troposphere, westerly winds dominate over the northern and central regions of India. Furthermore, a pattern of cyclones and anticyclones emerges within the latitude belt of 10-40°N across Indian longitudes. Specifically, an anomalous mid-tropospheric anticyclone induces westerly wind anomalies over the head of the Bay of Bengal (BoB). In the equatorial regions during MAM 2024, upper tropospheric winds exhibit

considerable strength over the western equatorial areas, whereas they appear weaker over the eastern equatorial zones.

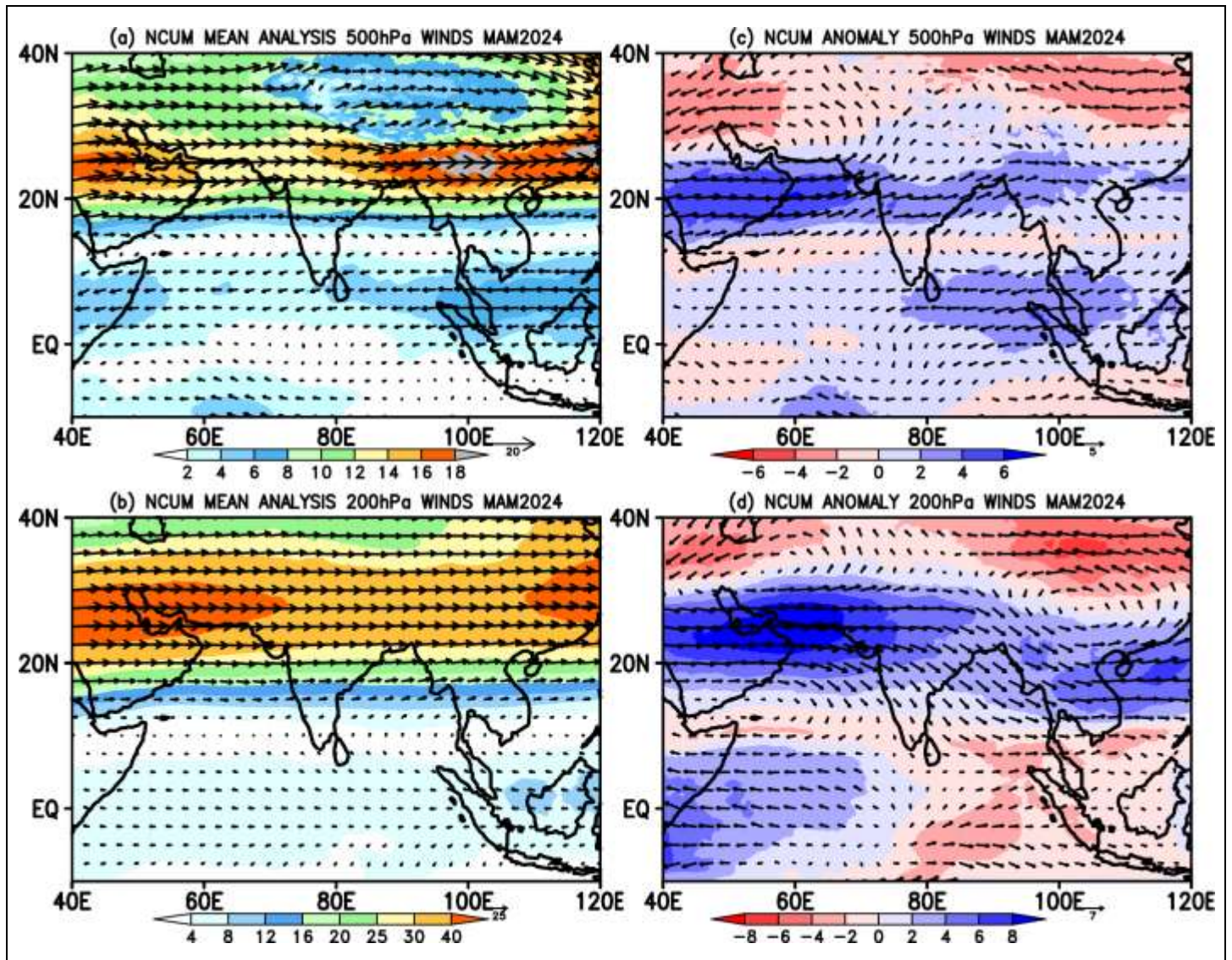


Figure 2. Mean winds at (a) 500 hPa and (b) 200 hPa in the NCUM-G Analysis during MAM 2024 (m/s). Right panels show the anomaly circulations at (c) 500 hPa and (d) 200 hPa.

3.2. Temperature at 850, 700, 500, and 200 hPa levels

The spatial distribution of seasonal mean temperature is shown in Figure 3. The mean daily temperature at the lower level (i.e., at 850 hPa) exceeds 20°C across the Indian land region and adjoining Seas (Figure 3a). The anomalous temperatures in the lower troposphere (i.e., at 850hPa and 700hPa, Figures 3c and 3d) indicate the Pre-monsoon season during 2024 is warmer than the climatology with magnitudes between 1^o to 2^oC over the Indian land region, excluding some parts of west of the north-western Indian region. The warmer temperatures

stretch from northwest to southeast India, covering the Indo-Gangetic plains (IGPs). The oceanic regions surrounding the Indian region are anomalously warm with uniform magnitudes ranging between 1-2°C, except for the northern Arabian Seas (AS). Nevertheless, the temperature anomalies across India still indicate warmer than the climatology at both 500 and 200 hPa levels.

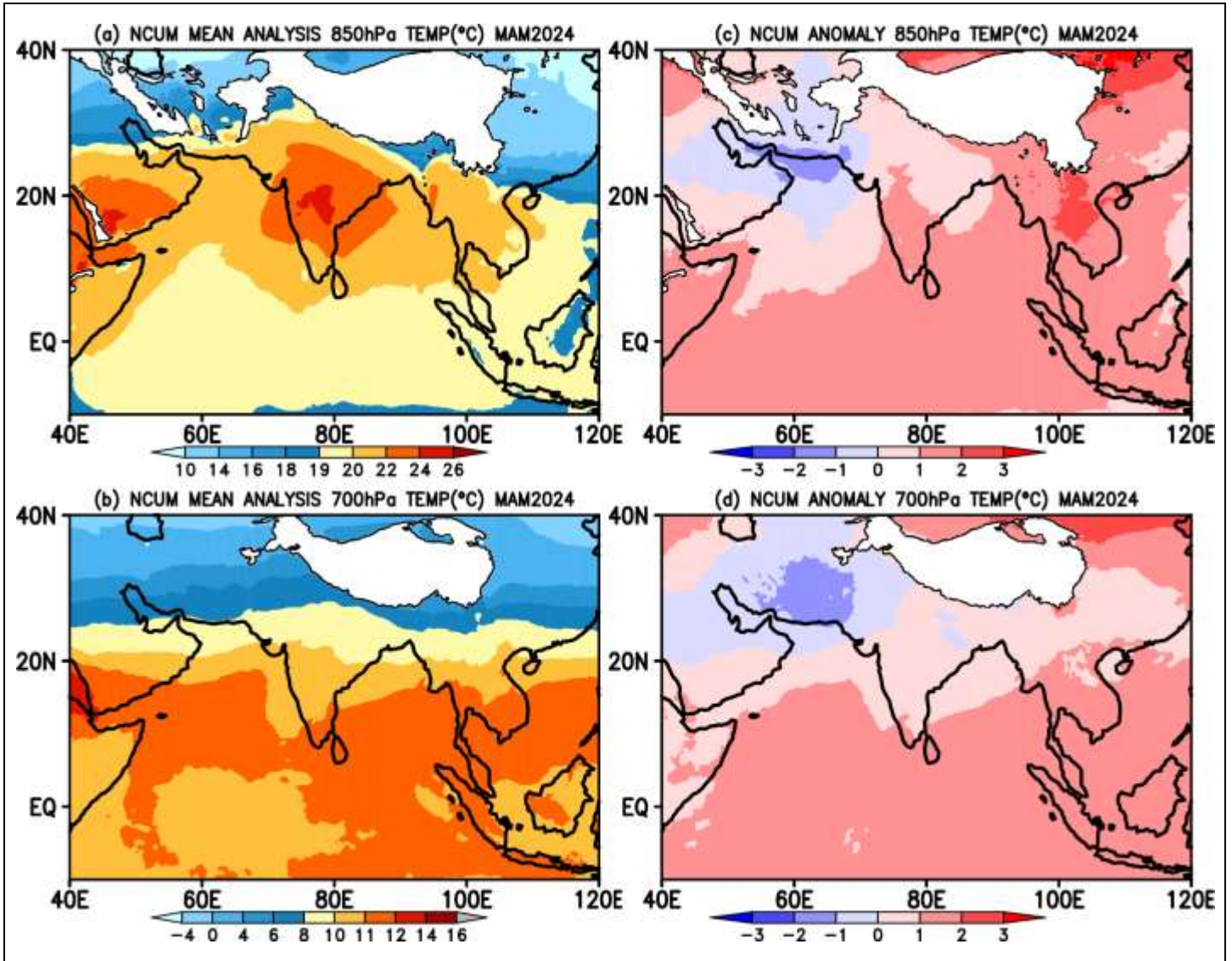


Figure 3. Mean Temperature (Degree Celsius, °C) at (a) 850 hPa and (b) 700 hPa in the NCUM-G Analysis during MAM 2024. Right panels show the Temperature anomalies at (c) 850 hPa and (d) 700 hPa.

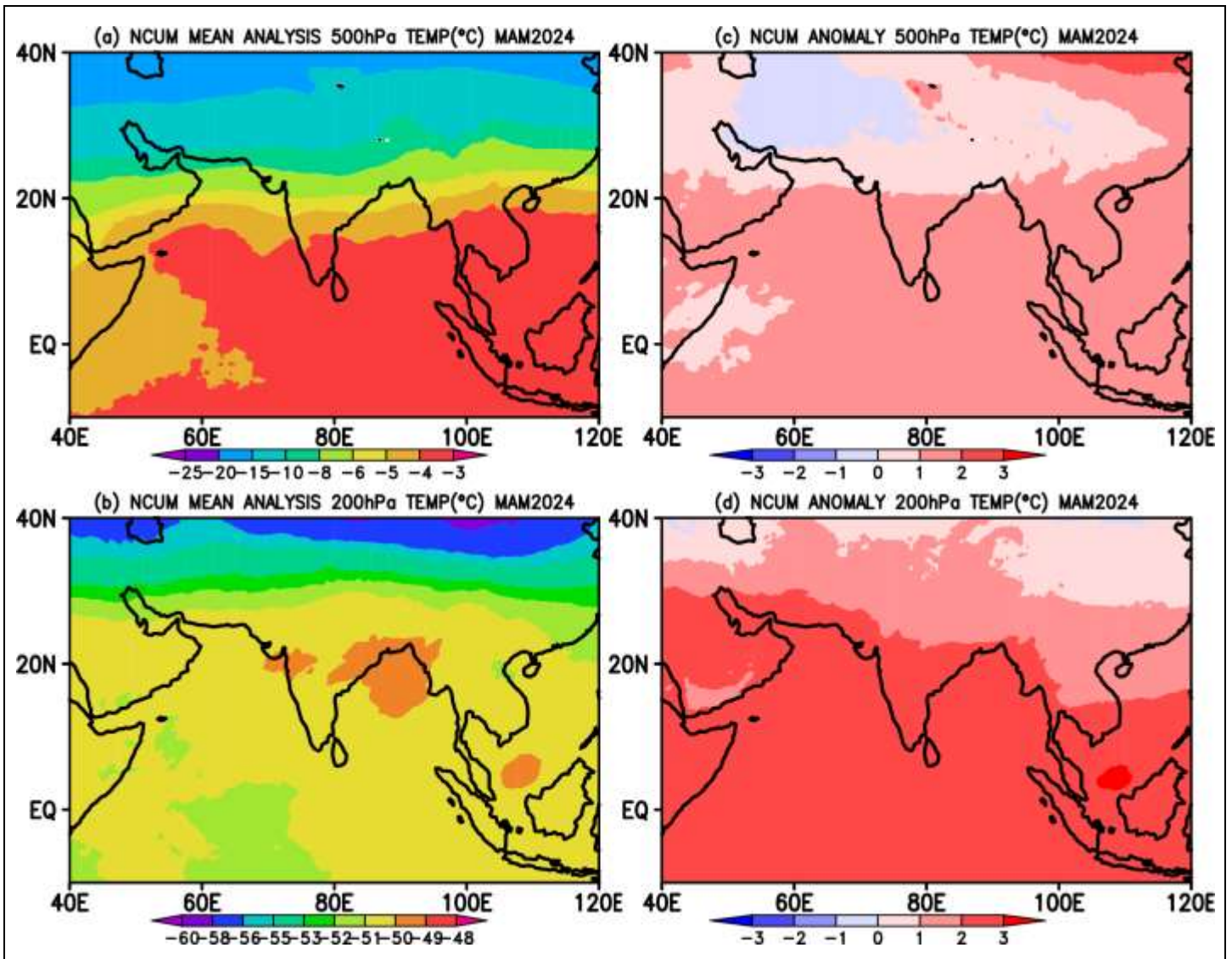


Figure 4. Mean Temperature (Degree Celsius, °C) at (a) 500 hPa and (b) 200 hPa in the NCUM-G Analysis during MAM 2024. The right panels show the Temperature anomalies at (c) 500 hPa and (d) 200 hPa.

3.3. Relative Humidity (RH) at 850, 700, and 500 hPa levels

The spatial distribution of humidity is an important field along with wind and temperature for its influence on the rainfall. Hence, we further show the spatial distribution of seasonal mean RH from NCUM-G model analysis in Figures 5a (850hPa) and 5b (700hPa). Mean RH at 850 hPa shows higher values over the south relative to north India. At 700 hPa, the mean RH is found to be higher than 50% over the Indian land region, south of the equator, and around the South China Sea regions. Also, when we examine the anomalies of MAM 2024 indicates a higher percentage of RH compared to the climatology across India, excluding the IGPs. Over the oceans surrounding the

Indian subcontinent, positive anomalies are observed over the western oceanic region, including the AS, while negative anomalies are present over the eastern oceanic region, including the BoB at 850 hPa (Figures 5c). At 700 hPa, positive anomalies are noted over the oceanic region, except for the southern BoB.

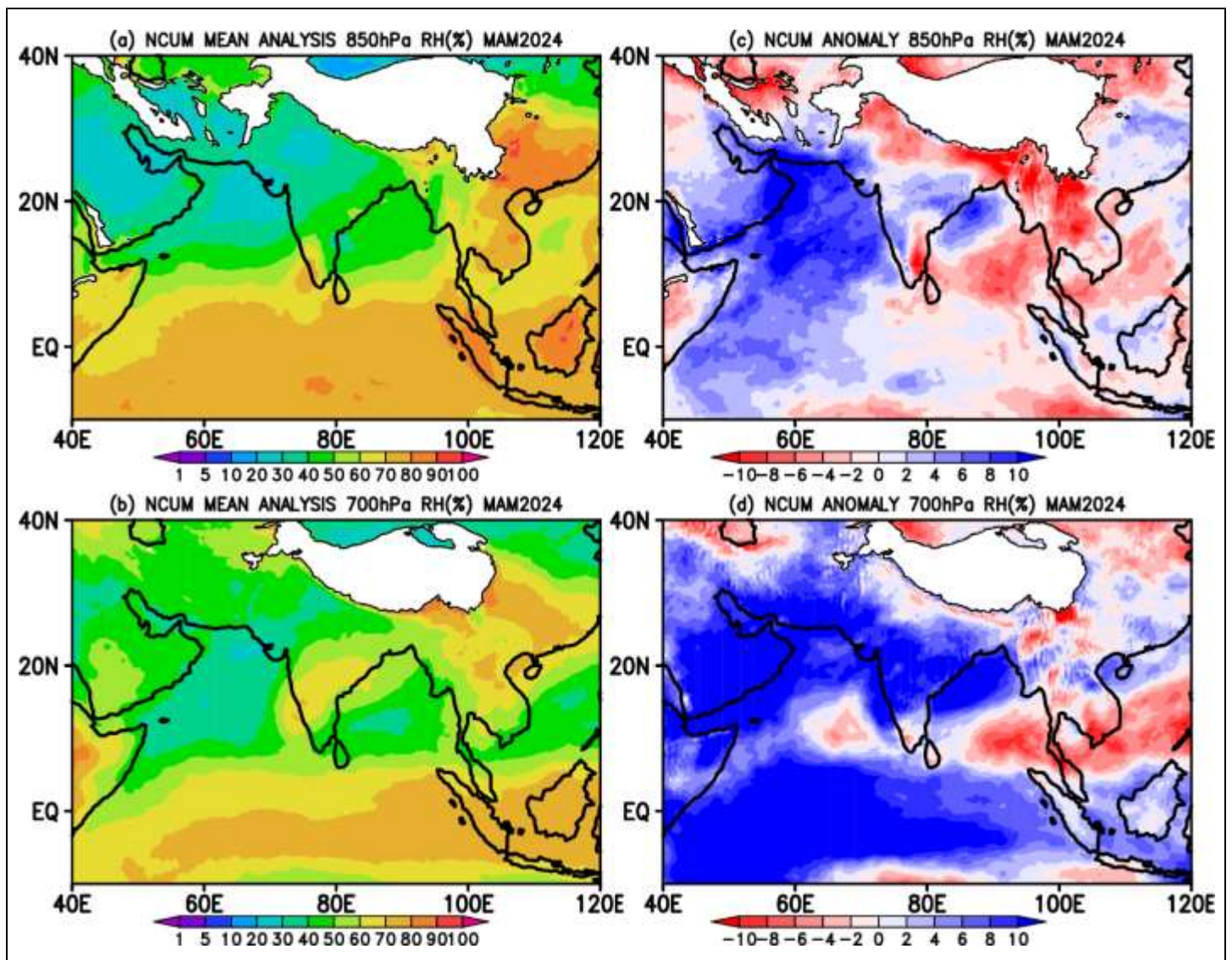


Figure 5. Mean Relative Humidity (%) at (a) 850 hPa and (b) 700 hPa in the NCUM-G Analysis during MAM 2024. The right panels show the anomalies in Relative Humidity at (c) 850 hPa and (d) 700 hPa.

Further, we also showed in Figure 6 the spatial distribution of RH in the mid-troposphere at 500 hPa level. The seasonal mean distribution of RH indicates dry conditions over the Indian subcontinent. Nevertheless, occasionally RH can be increased due to the movement of synoptic-scale disturbances in north India during Pre-monsoon. On the other hand, in the oceanic regions, specifically in the equatorial Indian ocean regions, maritime continent, a significant amount of the available moisture with RH magnitudes of more than 60% can be noticed. The anomalous RH distribution is shown in Figure 6 (right panel). The south Indian region shows positive

anomalies in RH with respect to climatology, but it may not be significant as the mean RH itself is extremely low. However, negative RH anomalies can be noticed over the maritime continent, where the mean distribution is generally higher.

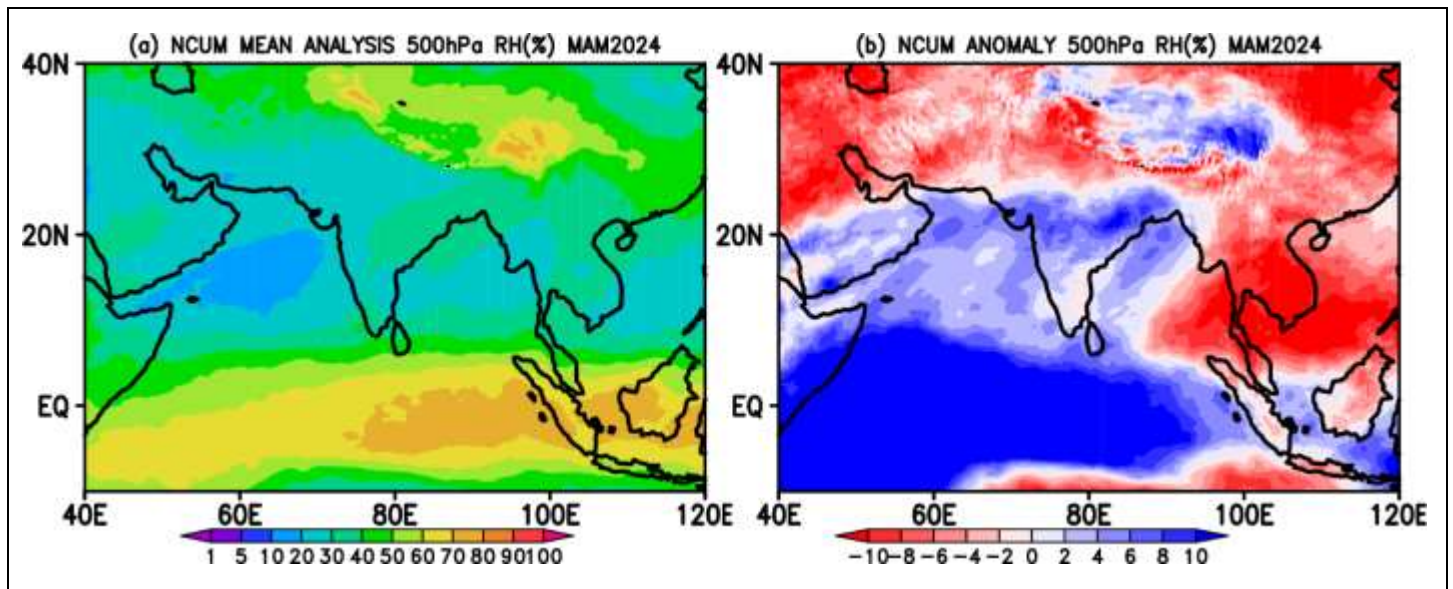


Figure 6: Mean Relative Humidity (%) at (a) 500 hPa in the NCUM-G Analysis during MAM 2024. The right panel shows the anomalies in Relative Humidity at (b) 500hPa.

4. Systematic Errors in NCUM-G Forecasts

This section briefly describes systematic errors in the Day-1 (24 hr), Day-3 (72 hr), and Day-5 (120 hr) forecasts during MAM 2024. The forecast errors with respect to model analysis are presented for Winds and Temperature at 850, 700, 500, and 200 hPa levels and Relative Humidity at 850 and 700 hPa levels (Figure 7-16).

4.1. Winds at 850,700, 500, and 200 hPa levels

The mean winds at the 850 hPa level indicate a ridge-type circulation over the central and northwestern regions of India, characterized by prevailing westerly and northwesterly winds. In the equatorial regions, mean westerlies dominate, with maximum wind speeds reaching approximately 4 m/s (Figure 7a). Systematic errors in the Day-1 forecasts at this level reveal a westerly wind bias over northern India, with enhanced northwesterlies along the west coast. These errors remain consistent across forecast lead times but increase in magnitude during the pre-monsoon season (Figures 7a-d). Similar patterns of systematic errors are observed at the 700 hPa level across the Indian region except the strong anticyclonic circulation is evident. Also, a more pronounced westerly wind bias is evident at the 700 hPa level over the western equatorial Indian Ocean in the Day-3 and Day-5 forecasts (Figures 8c-d).

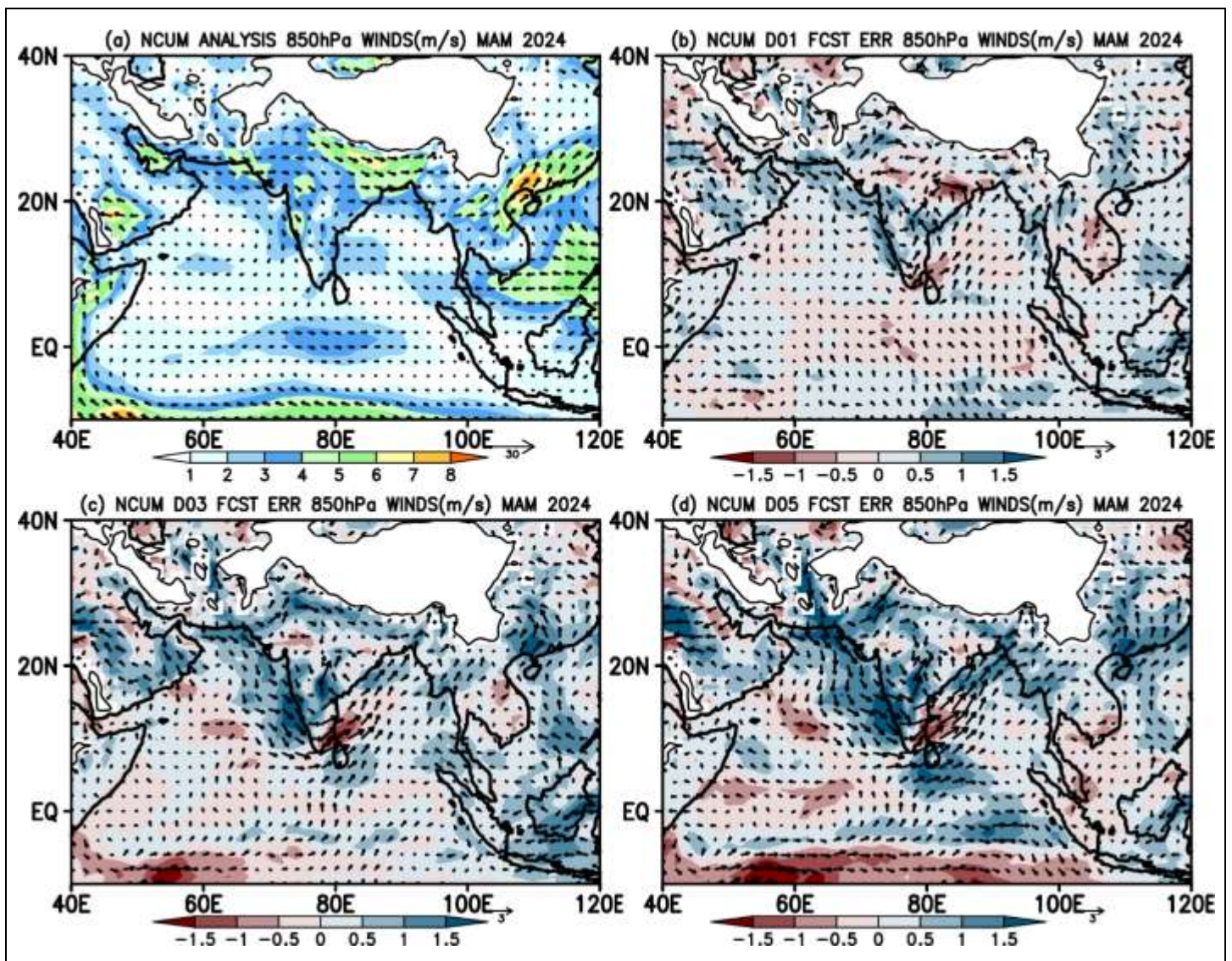


Figure 7. (a) Mean winds (m/s) and systematic errors (m/s) in (b) Day-1, (c) Day-3, and (d) Day-5 forecasts at 850 hPa during MAM 2024.

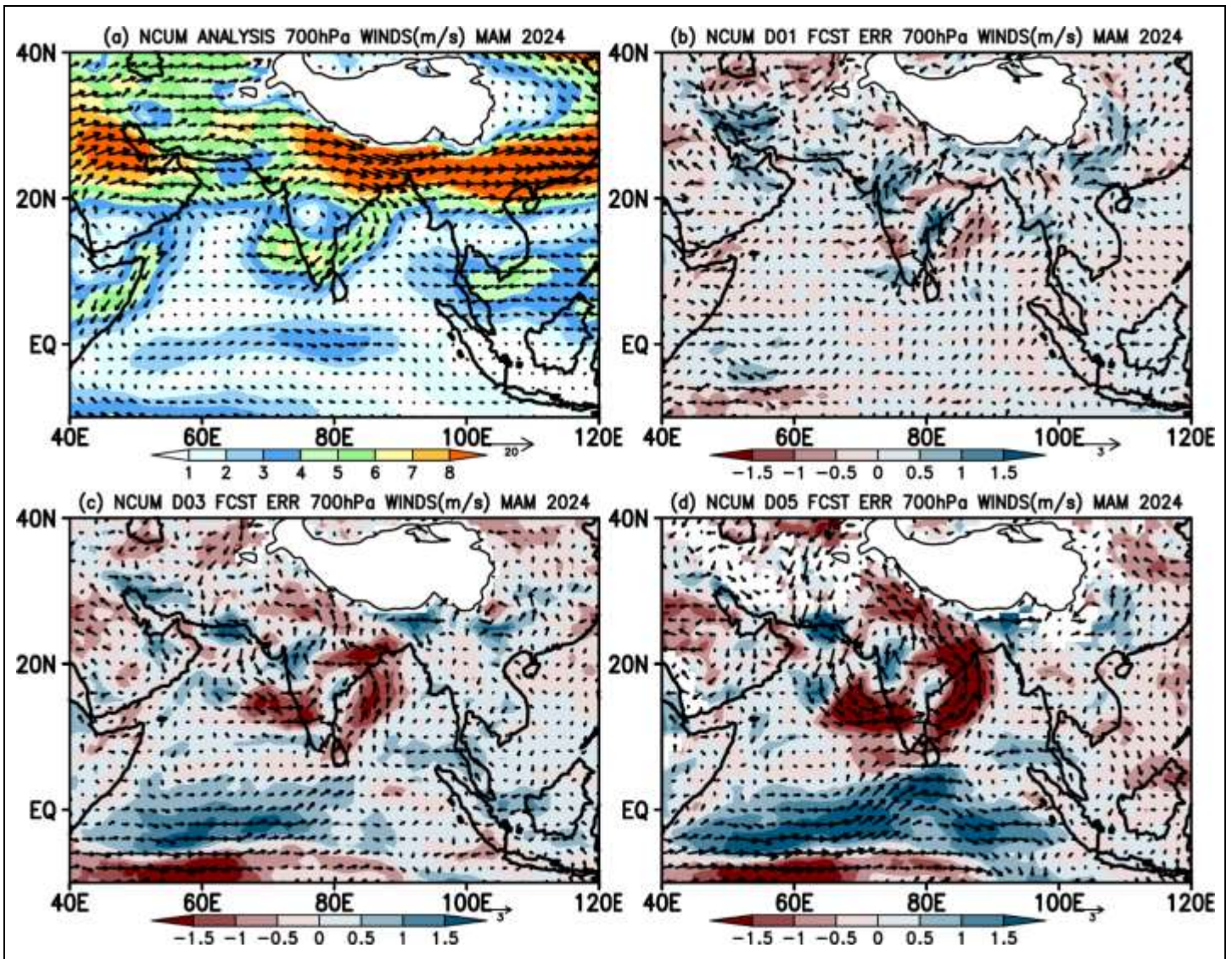


Figure 8. (a) Mean winds (m/s) and systematic errors (m/s) in (b) Day-1, (c) Day-3, and (d) Day-5 forecasts at 700 hPa during MAM 2024.

Mean winds at 500 hPa level show strong westerlies between 30-40° N, and these westerly winds penetrated over the north and central Indian region. Errors in winds at 500hPa level are relatively small in Day-1 forecasts. The south-easterly wind bias seen over northern parts of India and the westerly wind bias over the western equatorial Indian Ocean are enhancing in Day-3 and Day-5 forecasts. The enhanced westerlies exhibit cyclonic circulation just above the equator in Day-5 forecast around 500hPa level, which is noteworthy (Figures 9a-d). Systematic errors at 200 hPa level winds show enhanced divergent circulation centered over central India as seen in Day-3 forecasts, and this divergent circulation shifted westward in Day-5 forecasts with enhanced error magnitudes (Figure 10 c-d).

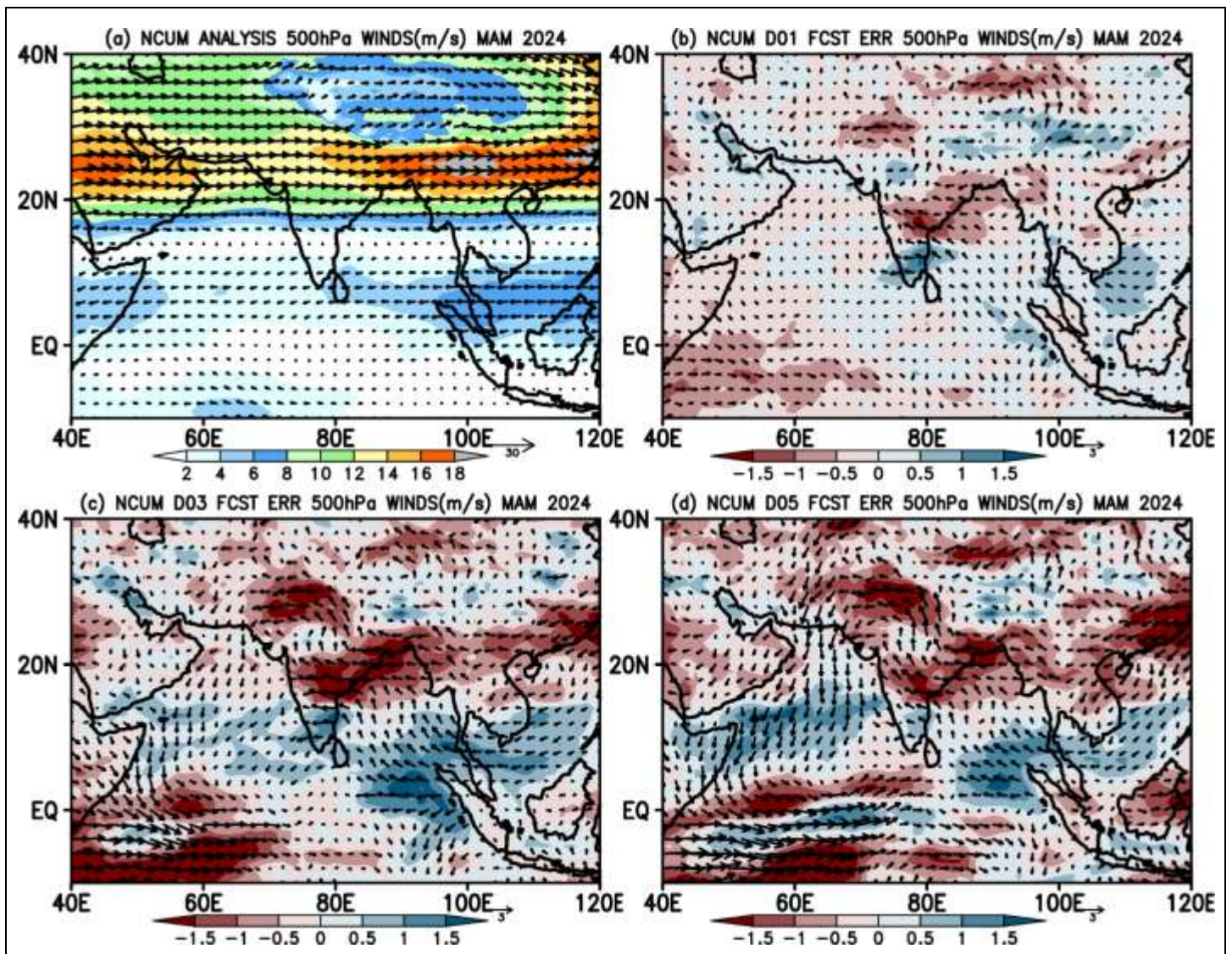


Figure 9. (a) Mean winds (m/s) and systematic errors (m/s) in (b) Day-1, (c) Day-3, and (d) Day-5 forecasts at 500 hPa during MAM 2024.

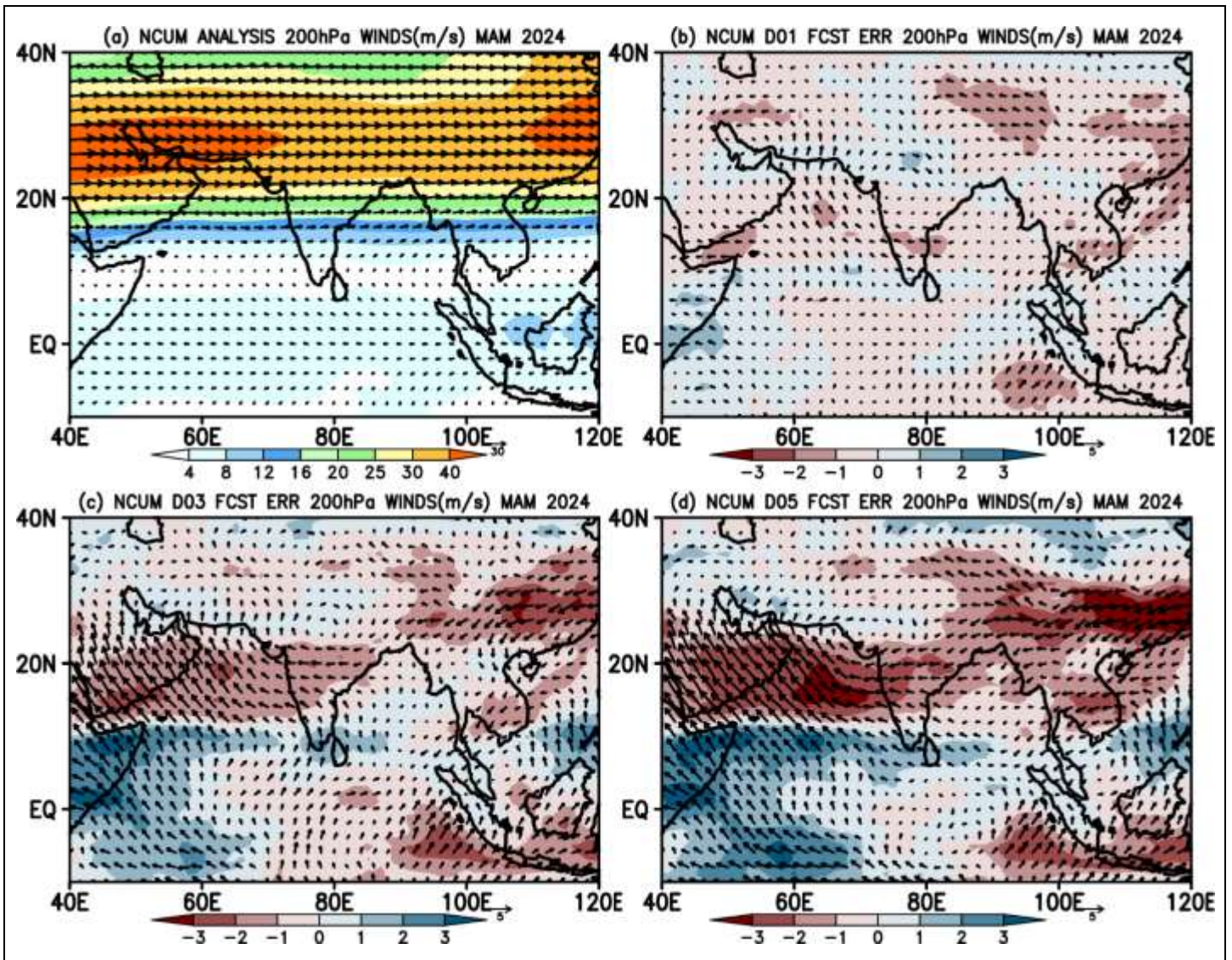


Figure 10. (a) Mean winds (m/s) and systematic errors (m/s) in (b) Day-1, (c) Day-3, and (d) Day-5 forecasts at 200 hPa during MAM 2024.

4.2. Temperature and Relative humidity

Spatial map of seasonal mean temperature from NCUM-G analysis at 850 hPa shows warm temperatures (20–22°C) over BoB and AS (Figure 11a). In particular, the central and southern peninsular regions of India indicated warmer temperatures than the adjoining oceans. The model shows warm bias ranging from ~0.5–1°C occupied over most of the Indian land mass, and the magnitude of this bias is increasing with forecasts lead time (Figures 11 b-d). These error increments at 850hPa temperatures are also more prominent over the Indo-Gangetic plain regions. On a similar note, the temperature at 700 hPa (Figure 12) also shows warm bias (>1°C) over most of the Indian land region. It is interesting to see that the bias over the south BoB region reverse sign and now exhibits cold bias compared to the 850hPa level. This cold bias over south BoB is seen in Day-3 and Day-5 forecasts. The Arabian Sea (AS) region also exhibits slight warming in all the forecast days, i.e., from Day-1 to Day-5 (Figures

12 b-d). At 500 hPa (200 hPa) level, temperature exhibits warm (cold) bias over the Indian land region, including surrounding oceanic regions, and the magnitude of the bias is increasing in forecasts with lead time (Figures 13 b-d (Figures 14 b-d)). Furthermore, a warm bias is observed at 500 hPa over the western Arabian Sea and the surrounding regions. at 200 hPa most of the region surrounding AS is cold except the northwestern India and the adjoining areas forecasts. This bias becomes more pronounced in Day-5 forecasts (Figures 13 b-d and Figures 14 b-d).

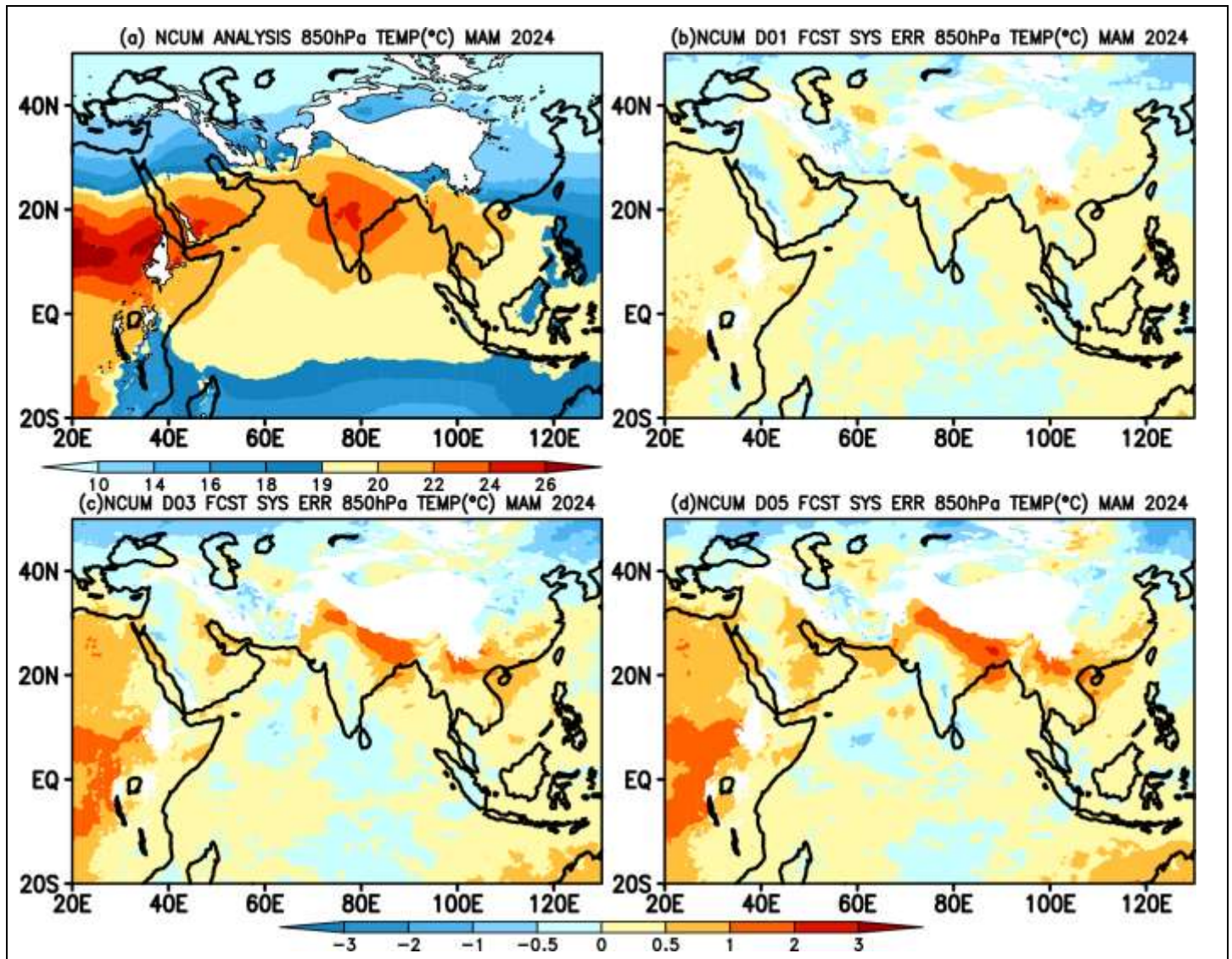


Figure 11. (a) Mean Temperature (Degree Celsius, °C) and systematic errors (Degree Celsius, °C) in (b) Day-1, (c) Day-3, and (d) Day-5 forecasts at 850 hPa during MAM 2024.

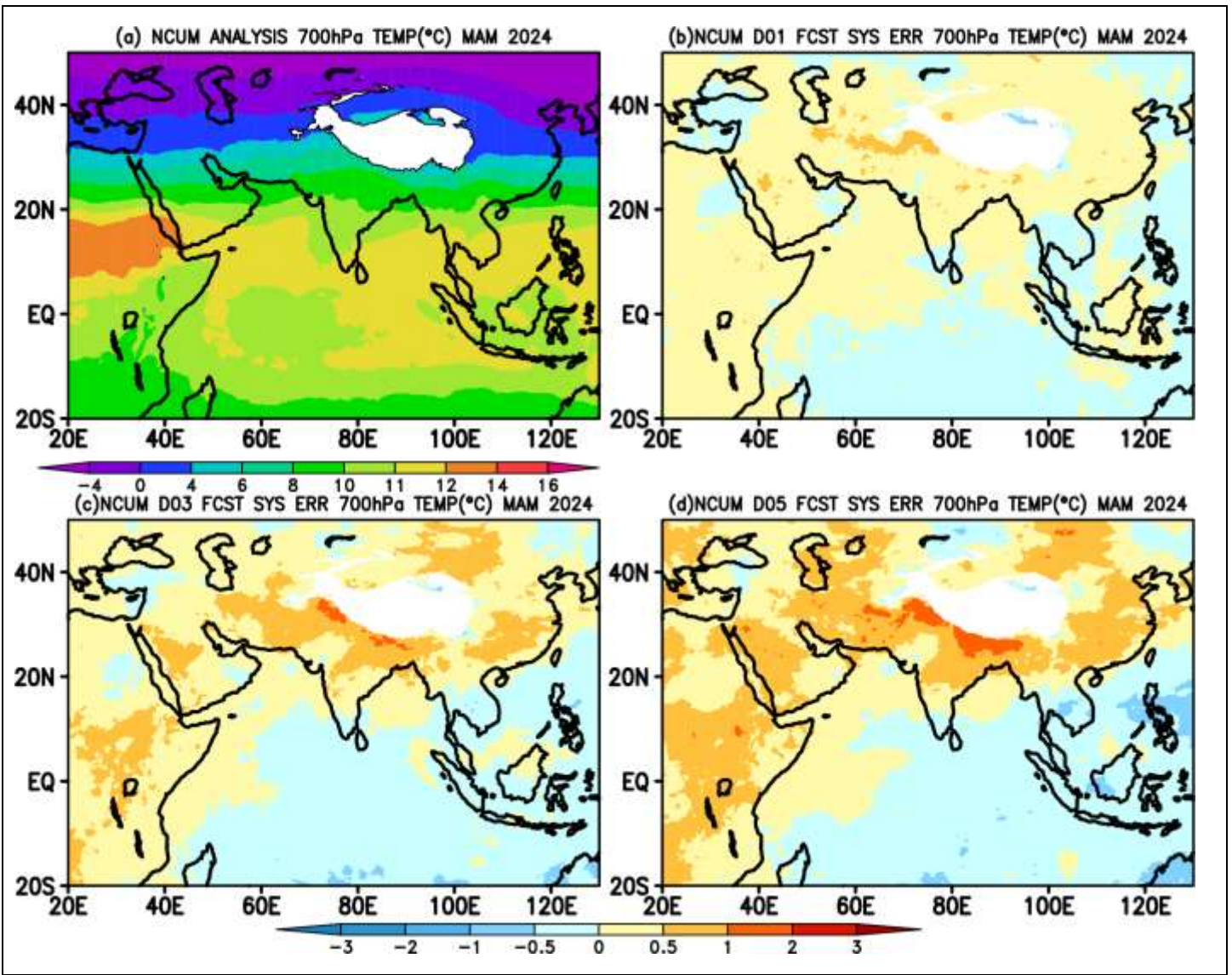


Figure 12. (a) Mean Temperature (Degree Celsius, °C) and systematic errors (Degree Celsius, °C) in (b) Day-1, (c) Day-3, and (d) Day-5 forecasts at 700 hPa during MAM 2024.

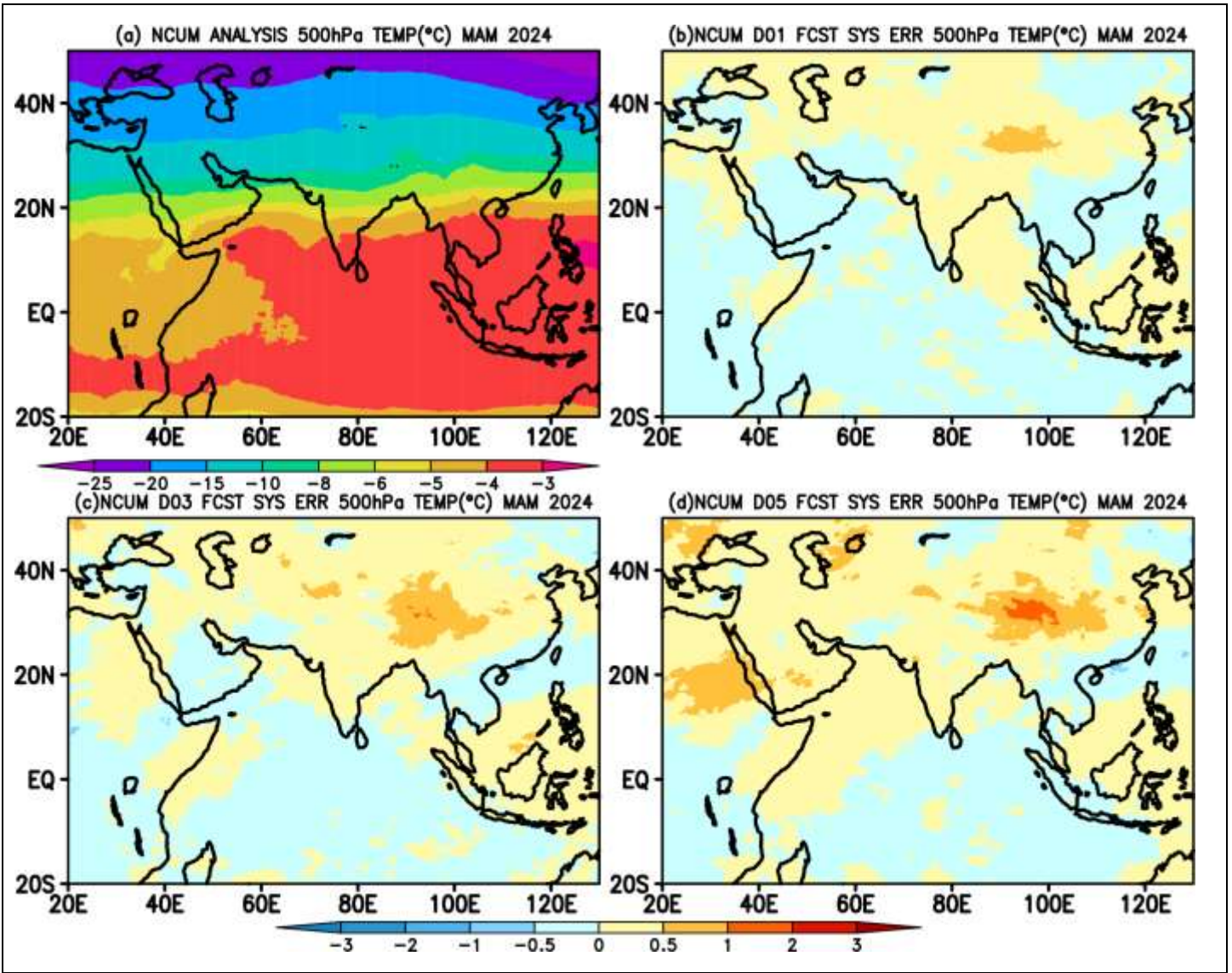


Figure 13. (a) Mean Temperature (Degree Celsius, °C) and systematic errors (Degree Celsius, °C) in (b) Day-1, (c) Day-3, and (d) Day-5 forecasts at 500 hPa during MAM 2024.

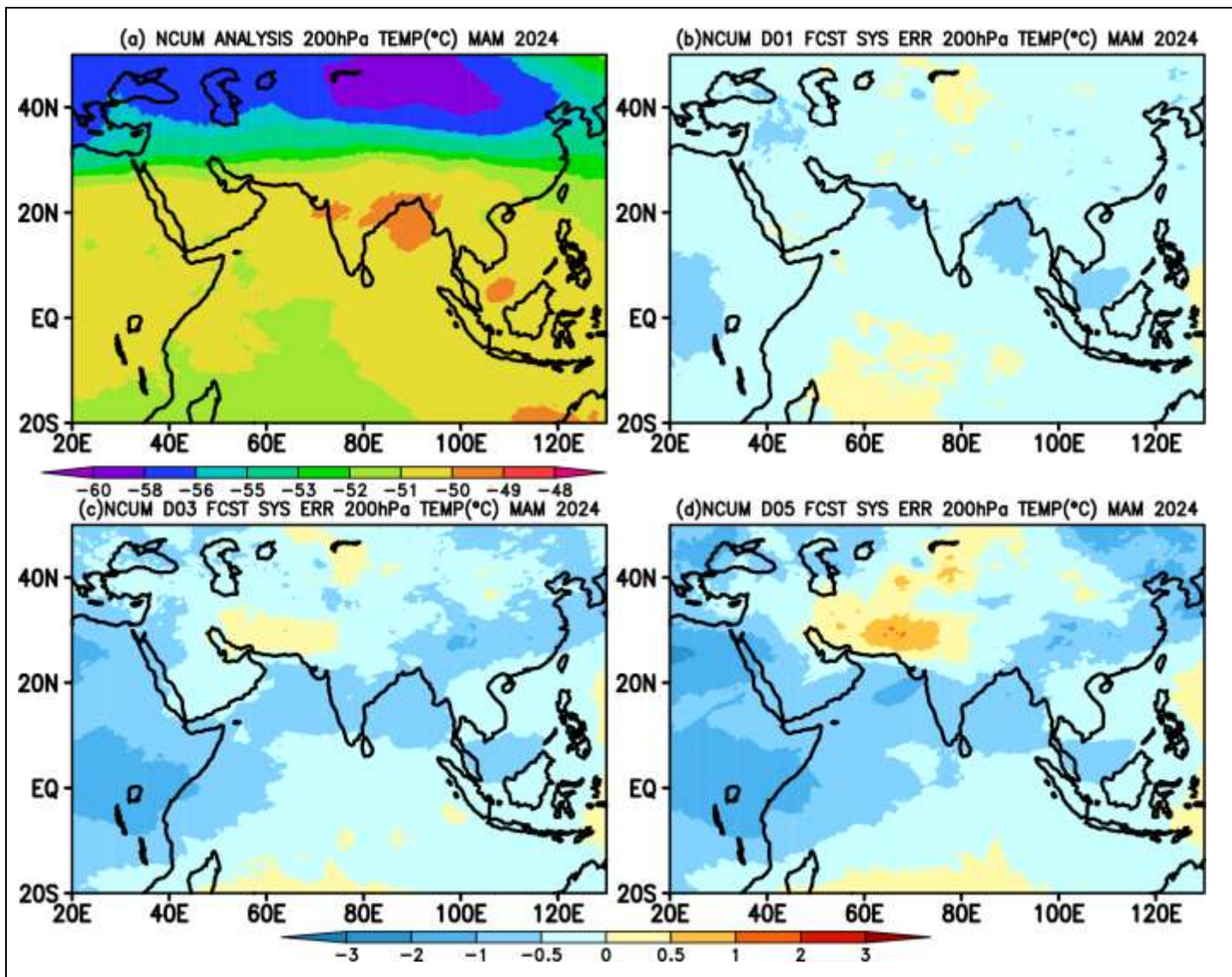
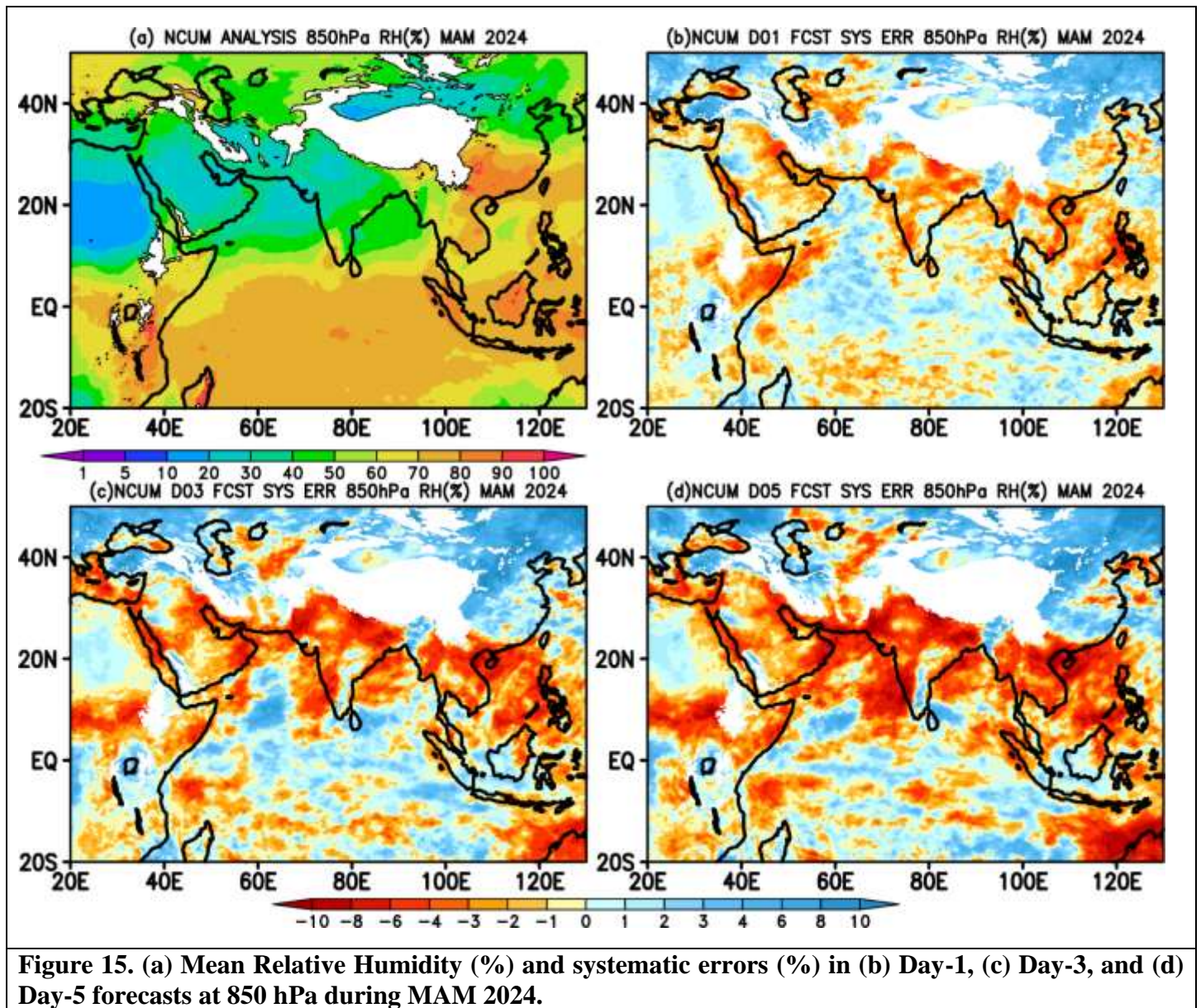


Figure 14. (a) Mean Temperature (Degree Celsius, °C) and systematic errors (Degree Celsius, °C) in (b) Day-1, (c) Day-3, and (d) Day-5 forecasts at 200 hPa during MAM 2024.

Seasonal mean RH at 850 (Figure 15) and at 700 hPa (Figure 16) levels show large values $> 80\%$ over the south of the equator and around South China Sea regions; and relatively lower RH values over the Northern parts of the Indian subcontinent. Systematic errors show a large dry bias over a majority of the Indian subcontinent at 850 hPa level, and the dryness is enhancing with forecast lead time (Figures 15 c-d). The presence of low-level anticyclone over the Indian sub-continent induces enhanced warming, which could be one primary reason for the negative RH values over the central Indian region (Figures 15c-d). However, parts of AS and BoB are exhibiting moist compared to other regions. Interestingly the dry bias seen in the lower levels over the Indian subcontinent enhances in magnitude at 700 hPa level (Figures 16 b-d). In contrast the regions south of the equator is more moist at this pressure level.

In the next section, a brief description of systematic errors in the model forecasts is presented for key surface variables such as 2m Temperature (Figure 17), 10m winds (Figure 18), and Total Precipitable water (PWAT; Figure 19). The errors are computed against the NCUM-G analysis.



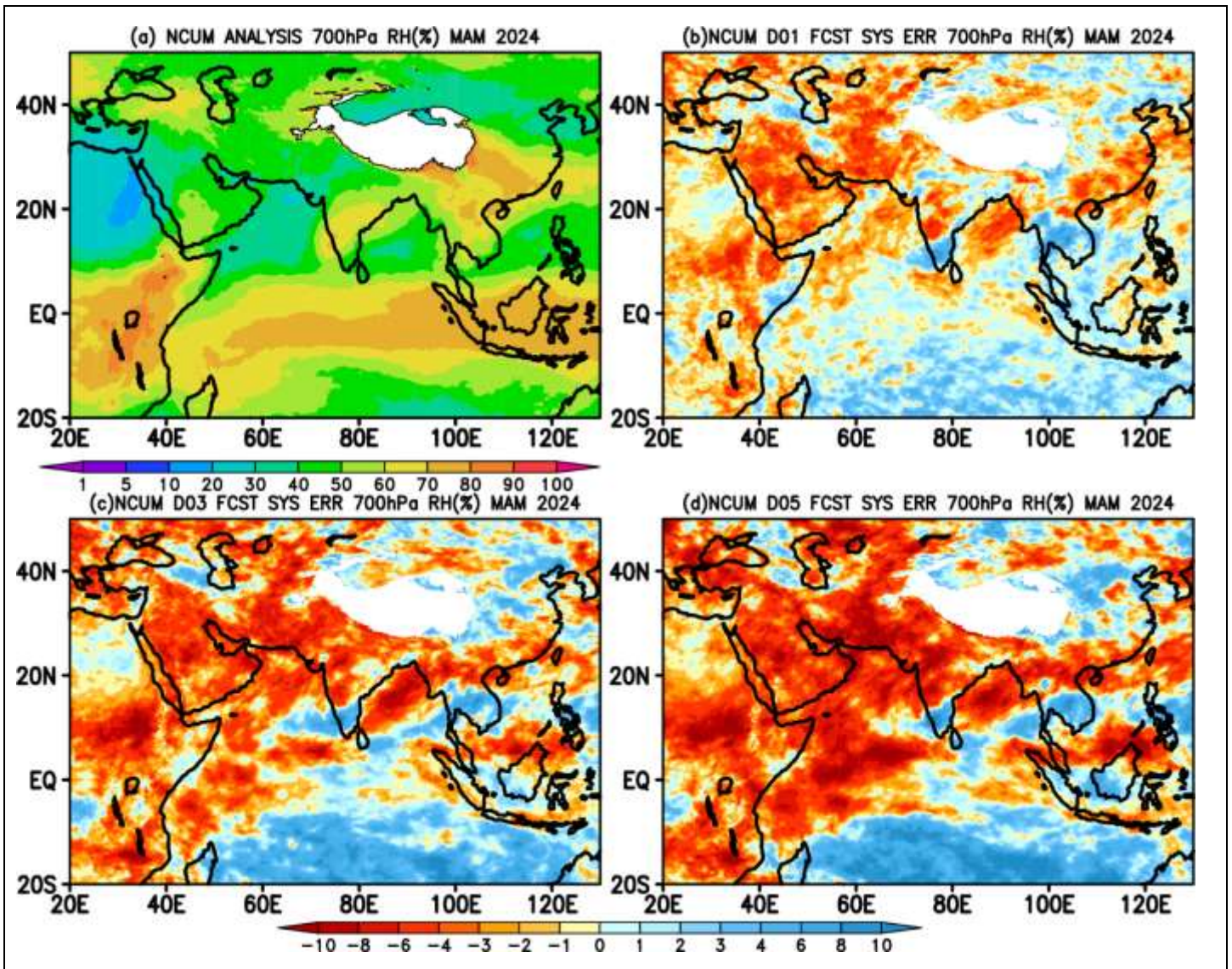


Figure 16. (a) Mean Relative Humidity (%) and systematic errors (%) in (b) Day-1, (c) Day-3, and (d) Day-5 forecasts at 700 hPa during MAM 2024.

4.3. Surface (10m) winds

Seasonal mean winds at 10m from the analysis show the presence of relatively strong north-westerlies over the AS, south-westerlies over head BoB, and weak westerlies over the tropical Indian Ocean (TIO), while strong easterlies south of TIO around 80 °E. The systematic errors in the forecasts depict a few notable features; 1) The north-westerly wind bias along the west coast over the northern AS and south-westerly wind bias along the east coast over BoB in Day-1 forecast is enhancing its strength with forecast lead time. 2) On a similar note, the easterly wind biases seen in the Day-1 forecast around the equator and south of the equator close to the maritime continent, and its direction changes to westerly wind biases in the Day-5 forecast (Figures 17 b-d).

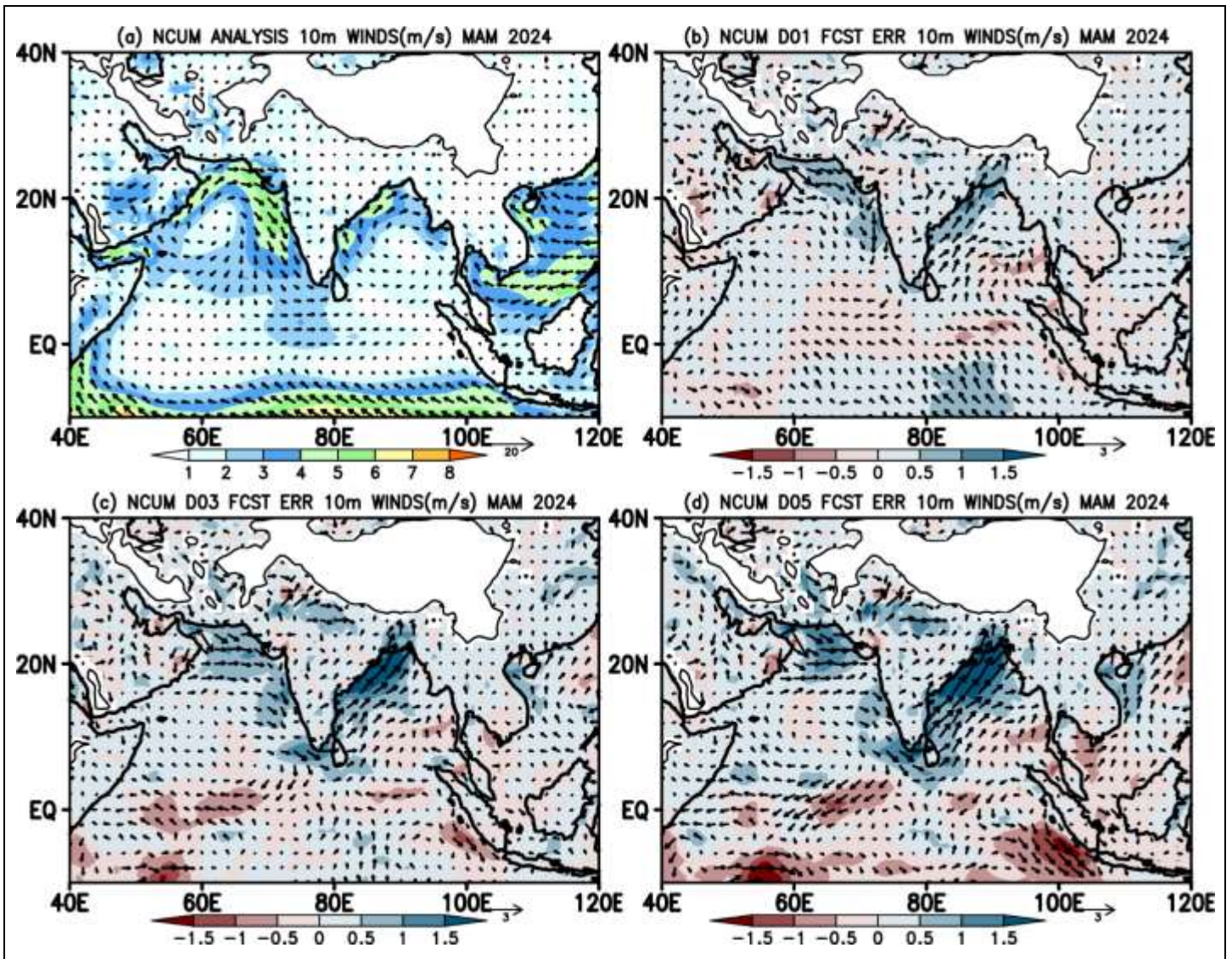


Figure 17. (a) Mean winds at 10m height and systematic errors (m/s) in (b) Day-1, (c) Day-3, and (d) Day-5 forecasts during MAM 2024.

4.4. Temperature at 2m

Seasonal temperature patterns over the Indian region show warm temperatures (33-40°C) on the Indian landmass and relatively cold temperatures over oceanic regions (Figure 18a). Systematic errors show a relatively warm bias over the Indian land regions and north of 40°N latitude regions. Interestingly these warm biases are increasing with forecast lead time, especially over the Indian region. This can be attributed to the dry north-westerly winds from the northwest entering Indian land and north AS (Figures 18 c-d). In addition, most of the oceanic regions of BoB and AS exhibited cold bias of the range $< -0.5^{\circ}\text{C}$ in all the forecast times. In addition, model temperature also exhibits a warm bias over the west of AS. It is noted that the magnitude of the bias is increasing with forecast lead time, which is noteworthy (Figures 18 c-d).

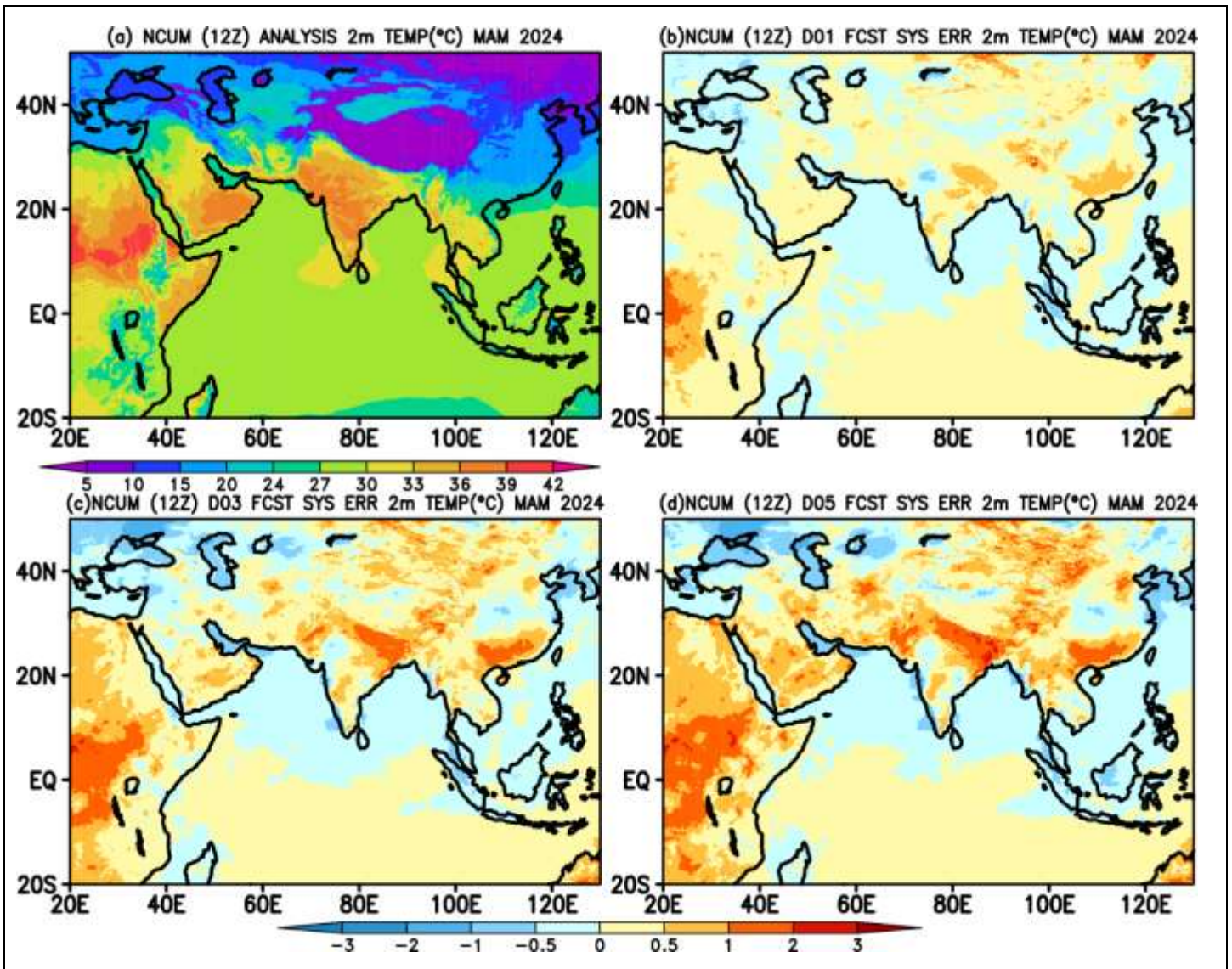


Figure 18. (a) Mean Temperature at 2m height and systematic errors (Degree Celsius, °C) in (b) Day-1, (c) Day-3, and (d) Day-5 forecasts during MAM 2024.

4.5. Total Precipitable Water (PWAT)

Seasonal mean PWAT shows a large value (> 60 mm) around the equatorial regions, especially over the Maritime Continent (MC), owing to the presence of a warm pool and associated convection during the pre-monsoon season over these regions. In contrast, most of the northern and central Indian regions are dry with very low PWAT values (5-15 mm). However, extreme southeast peninsular India exhibits moderate PWAT values around 35-40 mm due to the westerly winds from the MC region (Figure 19a). Systematic error in PWAT shows a column dry over Indian land regions in the Day-1 forecast; this dryness in the column is enhanced with forecast lead time, and its magnitude is maximum in the Day-5 forecast (Figures 19 c-d). Moderately positive PWAT bias is seen over the south of equatorial regions.

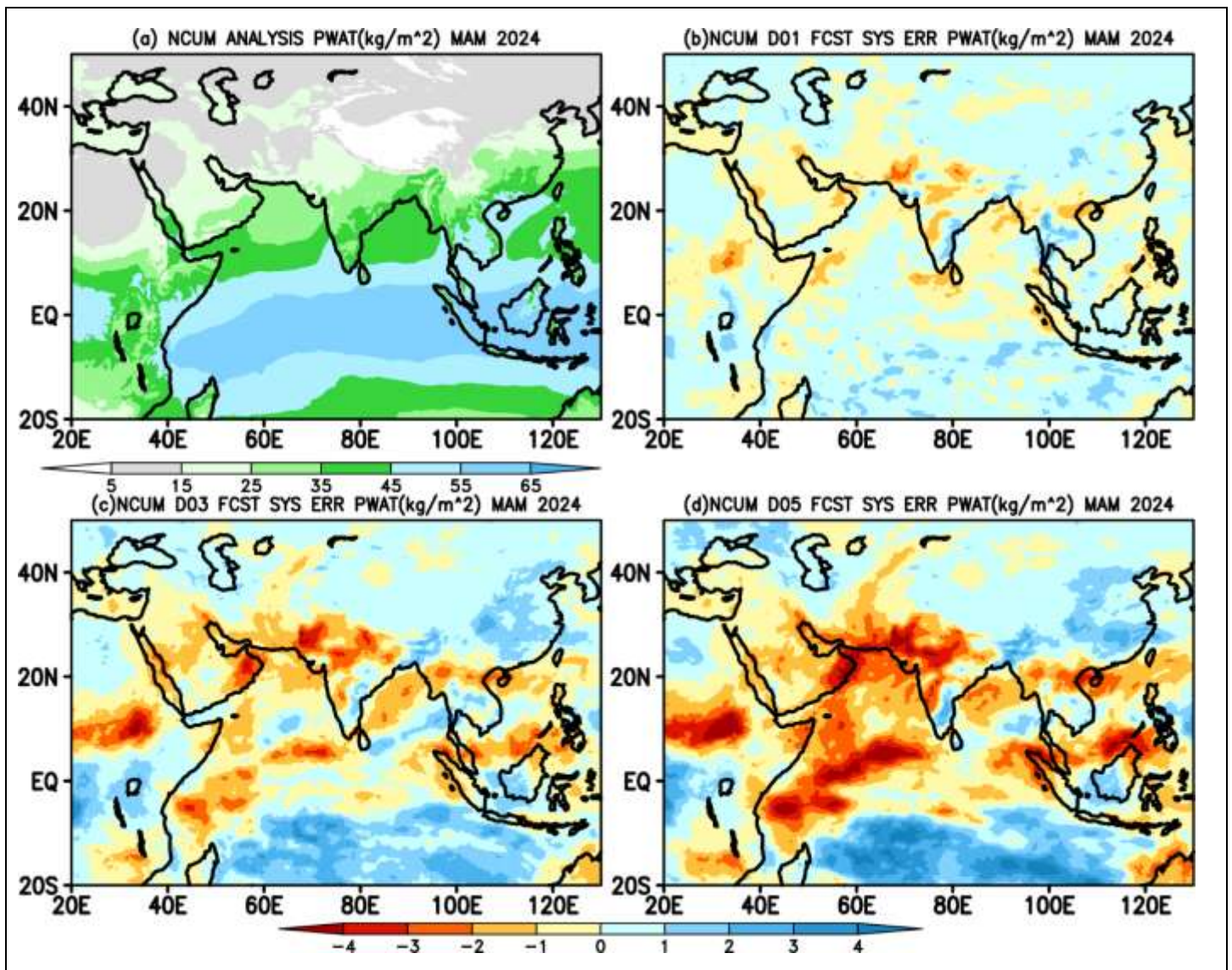


Figure 19. (a) Mean precipitable water content (PWAT) up to model levels and systematic errors (mm) in (b) Day-1, (c) Day-3, and (d) Day-5 forecasts during MAM 2024.

5. Forecast Verification during MAM 2024

Verification of NCUM-G model rainfall forecasts is presented in this section for MAM 2024. The daily accumulated rainfall forecasts are verified against the NCMRWF-IMD merged satellite and gauge rainfall product. The discussion presented in this section is confined to mean and mean error (ME) over the India region. Further, this section also quantifies forecast skill using standard verification metrics, namely, the probability of detection (POD), false alarm ratio (FAR), and critical success index (CSI), which are described in standard textbooks (Wilks, 2011, Jolliffe and Stephenson, 2012); and Symmetric extremal dependence index (SEDI), a metric for extreme and rare events (Stephenson et al 2008, Ashrit et al 2015b, Sharma et al 2021).

5.1. Rainfall Mean and Mean Error

The observed and forecast mean rainfall during MAM 2024 is shown in Figure 20. Observations indicate that most of the Indian subcontinent is dry in this season. However, we can notice the rainfall amounts over the northern parts of India that are associated with the disturbances/troughs from the west, which are termed as western disturbances (WDs). Moderate rainfall (2-4 mm/day) is also seen over southern parts of peninsular India, along the eastern coastal regions, and north-eastern regions (Figure 20a). The panels in the middle row, Figures 20 b-d, show the Day-1, Day-3, and Day-5 NCUM-G forecast rainfall averaged during the MAM2024 period. The observed rainfall regions are well predicted in all the forecast times. However, it is found that the NCUM-G forecast overestimates rainfall amounts over Kerala, along the eastern coastal and the north-eastern regions. Apart from this, most of the Indian subcontinent is dry with no convection in both observations and forecasts (Figures 20 a-d). Now, to further quantification, forecast mean errors (ME) are computed against the observation. The panels in the bottom row show rainfall ME (Figures 20 e-g) in predicted rainfall, indicating wet bias (blue) over north-eastern parts while dry bias off-coast of Kerala, Odisha, Tamil Nadu, and Myanmar regions. The magnitude of the dry bias increases with forecast lead time.

5.2. Categorical Scores of Rainfall Forecasts

To further quantify the model rainfall forecasts, categorical skill scores are computed over the Indian subcontinent. The categorical approach of verifying quantitative precipitation forecast (QPF) is generally based on the 2 x 2 contingency table, which is evaluated for each threshold. Verification scores are presented for rainfall thresholds of up to 30mm/day. For different rainfall thresholds, the probability of detection (POD) and the false alarm ratio (FAR) show a decrease and increase in scores, respectively. The BIAS score (frequency bias) indicates that forecasts overestimate the frequency at various thresholds. The values of Peirce's skill score (PSS) and the Symmetric extremal dependence index (SEDI) all are high for rainfall up to 3-6 mm/day, suggesting reasonable skill. PSS score shows a very sharp decrease as the threshold varies. Overall, the skill is not bias-free. For rainfall thresholds (> 10 mm/day), frequency bias is almost constant, but the skill is low, as indicated by the critical success index (CSI), PSS, and SEDI (Figure 21).

5.3. Categorical Scores of T_{max} at 2m

Similar analysis, as discussed in the above section, is repeated for maximum temperature thresholds. The POD slightly increases with the thresholds from 30°C to 44°C while the PSS score is nearly constant and below 0.3 till 40 °C, thereafter, it slightly increases to above 0.3. FAR scores over all India as a whole shows relatively large values >0.6 in all temperature thresholds and varies between 0.6-0.8 in all forecast lead times (Figure 22).

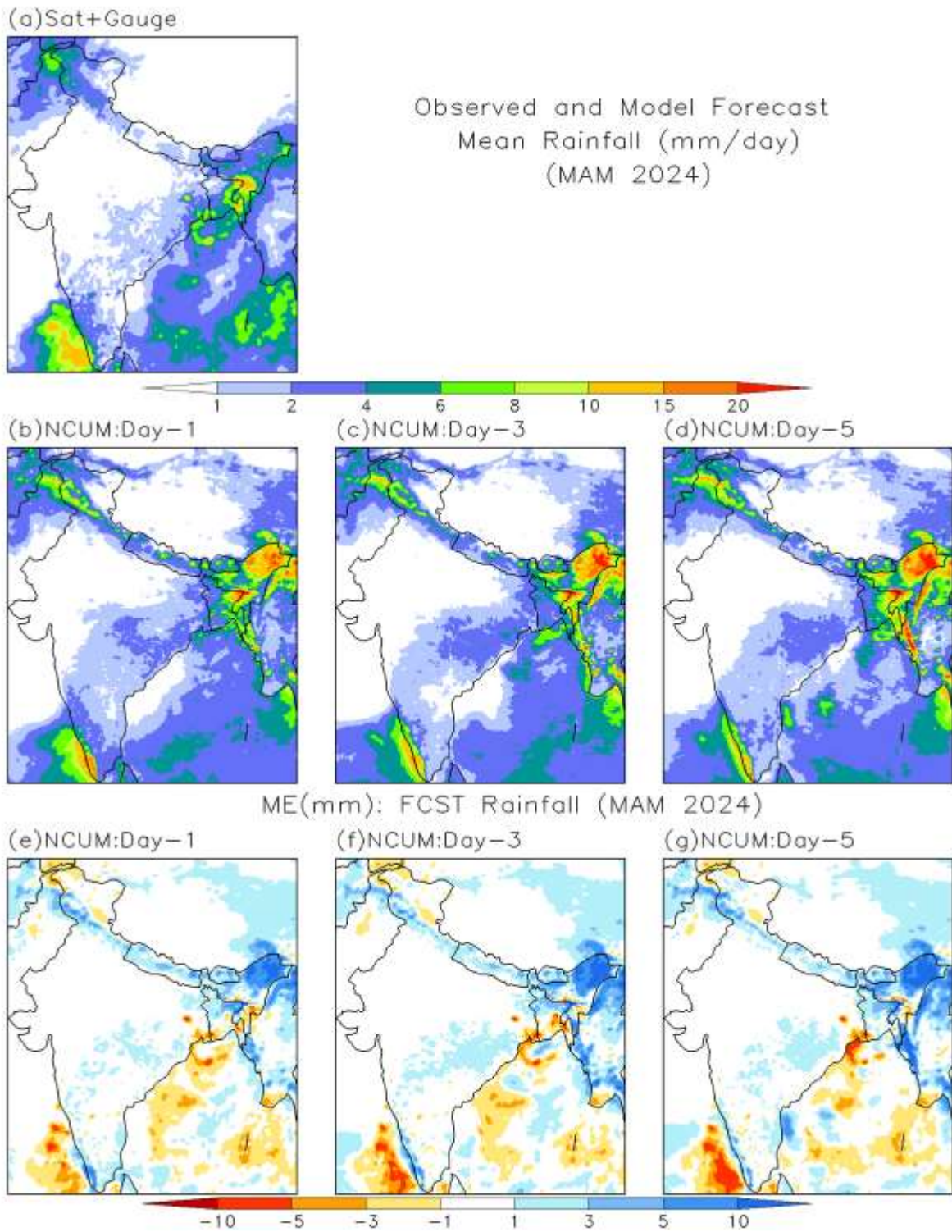


Figure 20. Accumulated MAM rainfall (mm) in (a) Observations and (b) Day-1, (c) Day-3, and (d) Day-5 forecasts. Bottom panels (e), (f), and (g) show Mean Error (ME) in Day-1, Day-3, and Day-5 forecasts, respectively.

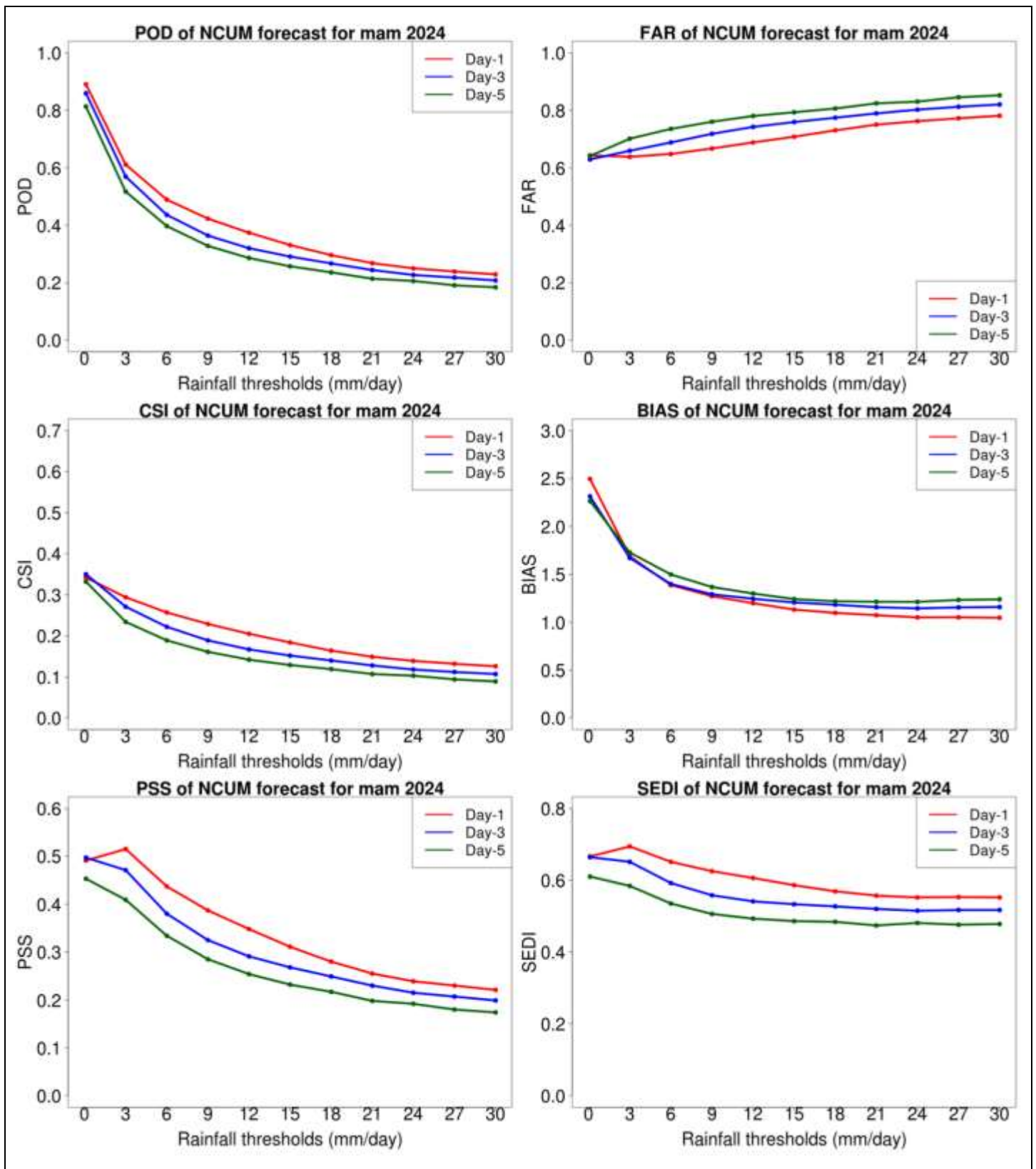


Figure 21. Categorical all India Rainfall scores POD (top left), FAR (top right), CSI (middle left), BIAS (middle right), PSS (bottom left), and SEDI (bottom right).

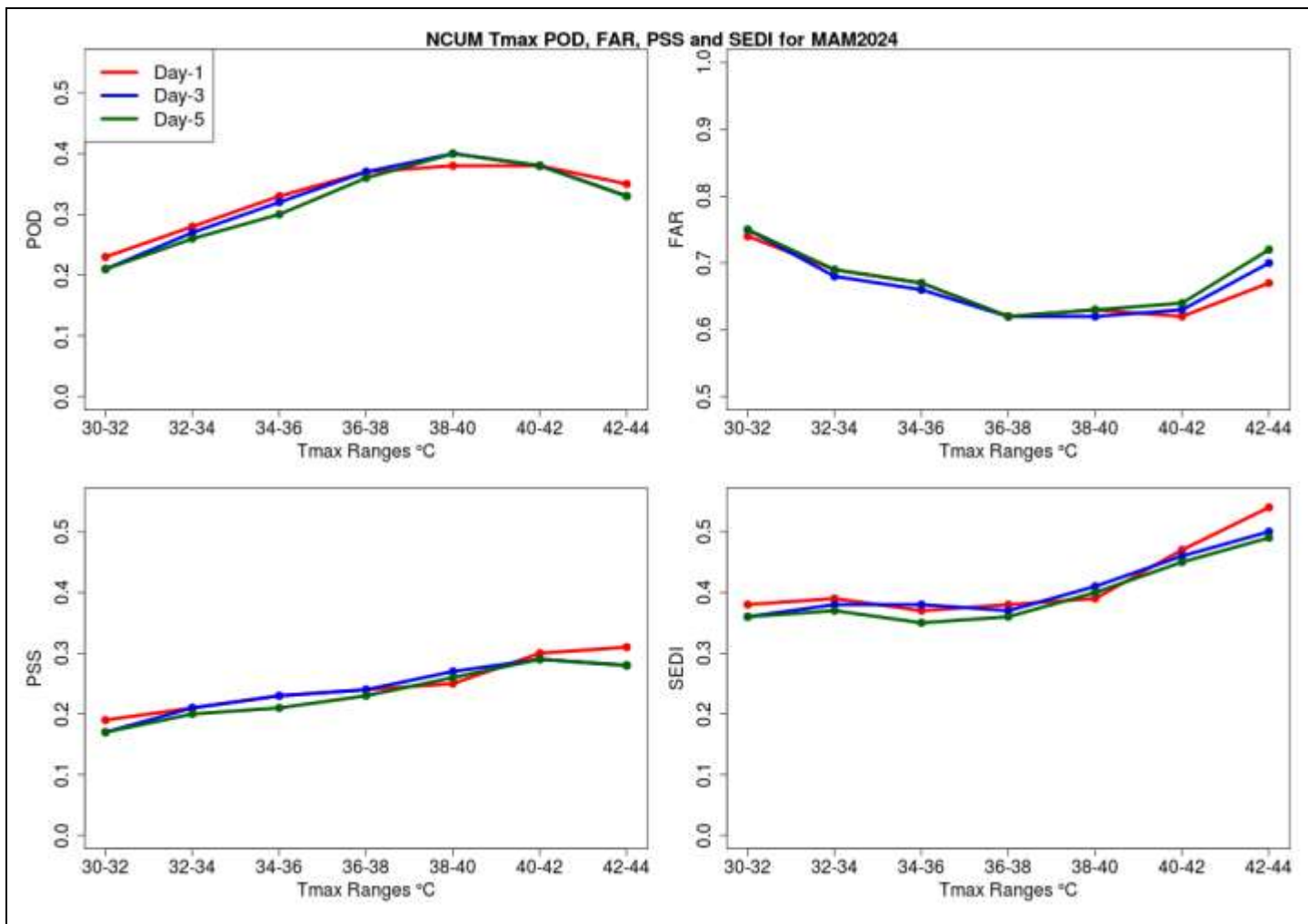


Figure 22. Categorical all India T_{max} scores POD (top left), FAR (top right), PSS (bottom left), and SEDI (bottom right).

6. Significant Weather during MAM 2024

This section summarizes the significant weather events, such as the cyclones, western disturbances, heat waves, extreme rainfall events, etc., that happened during the MAM2024 season along with the forecast assessment from the NCUM-G model.

6.1. Bay of Bengal SCS ‘REMAL’ during 24-28 May 2024

This section gives a brief summary report on the verification of the NCMRWF model forecasts for the recent Severe Cyclonic Storm (SCS) ‘REMAL’ during 24-28 May 2024, which developed over the Bay of Bengal (BoB). The SCS crossed Bangladesh and adjoining West Bengal coasts between Sagar islands and Khepupara close to southwest of Mongla near latitude 21.75°N and longitude 89.20°E between 22.30 hours IST/1700 UTC of 28th and 00.30 hours IST/1900 UTC of 27th May 2024. Verification of the forecast tracks and intensity is presented for all NCMRWF Unified Models; NCUM-G (12km grid resolution), NCMRWF Global Ensemble Prediction

System (NEPS-G; 12km grid resolution), and NCMRWF Regional Unified Model (NCUM-R; 4km grid resolution) for both 00UTC and 12UTC runs. Forecast verification is presented for model-predicted tracks and intensity against IMD best track data.

6.1.1. Forecast Tracks and Strike Probability

The observed and predicted tracks based on 00UTC of 26th May 2024 are shown in Figure 23 (top). All the predicted tracks indicated that SCS Remal would track towards the Bangladesh coast. The strike probability (Figure 23; bottom)) based on the 23 (1 control+22 perturbed) members of the NEPS-G ensemble, it also indicates that the cyclone would approach the coasts of Bangladesh and West Bengal.

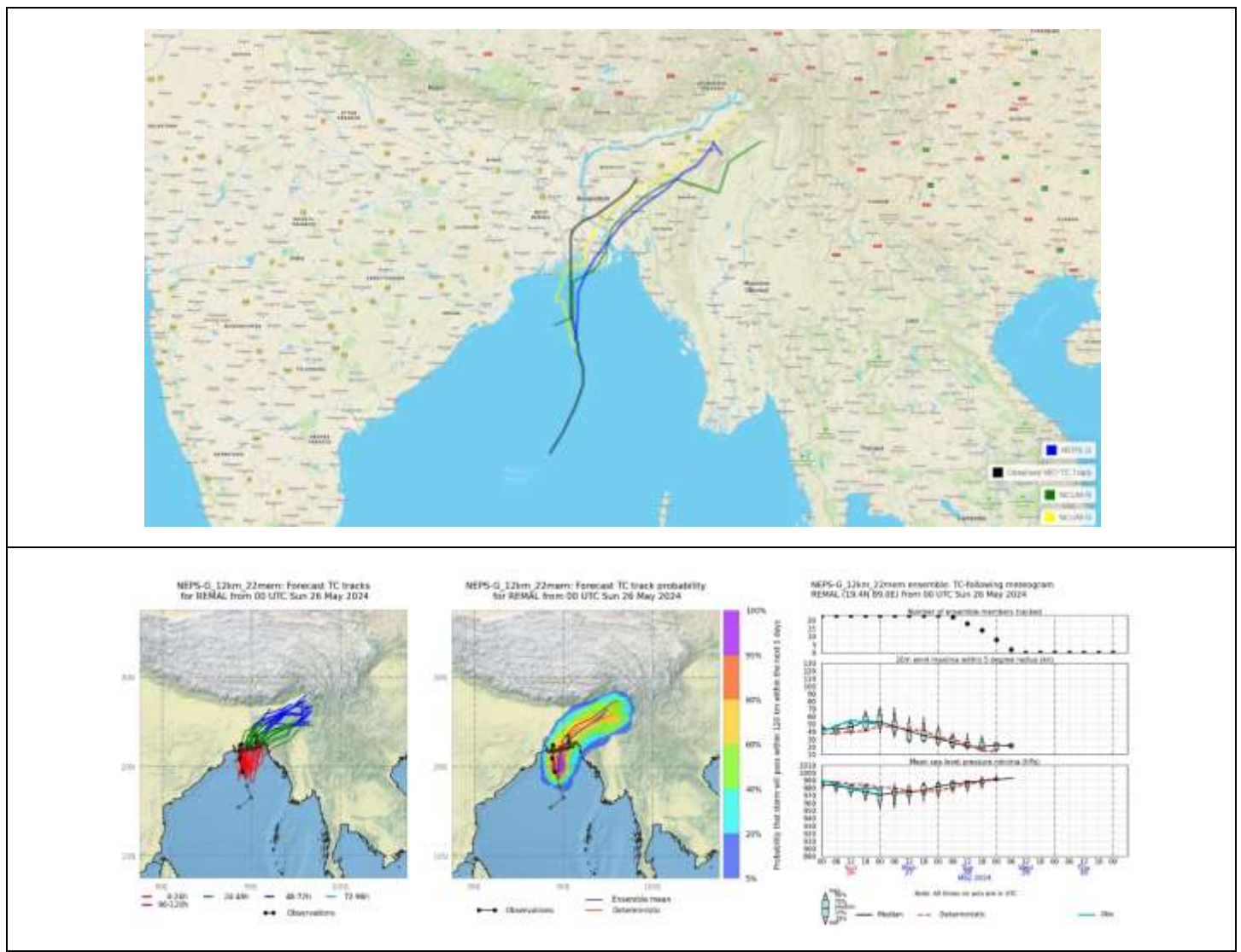


Figure 23. Observed & forecasted tracks of Bay of Bengal SCS ‘Remal’. Forecast tracks, strike probability, and EPS grams are based on IC 00UTC 26th May 2024.

6.1.2. Forecast Track Errors

The NCUM-G, NCUM-R, and NEPS-G model forecasts have been used in the verification. Forecast Verified since 19th May 12UTC for NCUM-G, 23rd May 12UTC for NEPS-G, and 23rd May 00UTC for NCUM-R. Table 1 summarizes the track errors of different models. The mean initial position error is the least (46 km) in NEPS-G, whereas the initial error is comparable (64 and 63 km) in both NCUM-G and NCUM-R models. NEPS-G features Direct Positional Error (DPE) <100 km up to 36 hrs.

The track error components, Direct Positional Error (DPE), Along Track Error (ATE), and Cross Track Error (CTE) are shown in Figure 24. ATE is highest in NCUM-R till 60 hr forecasts but least after 72 hours of forecast. On the other hand, CTE is larger in NCUM-G.

Table 1. Forecast Track Errors NCUM-R, NCUM-G, and NEPS-G (numbers in the adjacent column in italics indicate number of forecast points validated).

Fcst Hour	DPE					
	NCUM-R	No of Fcst verified	NCUM-G	No of Fcst verified	NEPS-G	No of Fcst verified
0	63	9	64	8	46	7
12	100	9	73	<i>10</i>	43	8
24	125	9	89	9	61	8
36	129	8	102	8	96	7
48	145	7	143	8	146	6
60	175	6	200	7	189	5
72	147	5	214	8	195	4
84			171	7	173	3
96			180	7	101	2
108			180	6	54	<i>1</i>
120			203	5	NA	0

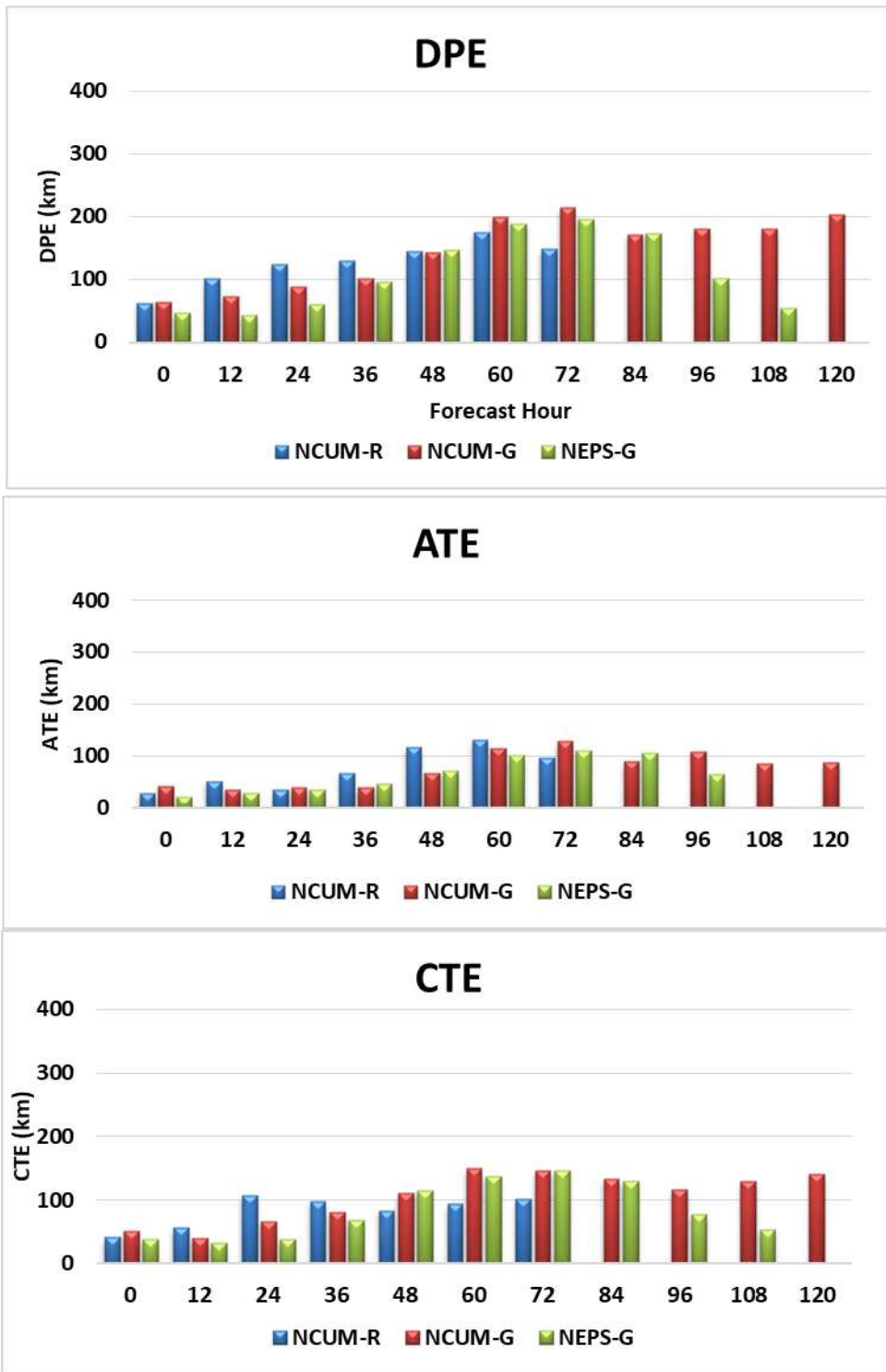


Figure 24. Track forecast errors (*top panel*) Direct Positional Error (DPE), (*middle panel*) Along Track Error (ATE), and (*bottom panel*) Cross Track Error (CTE) in km.

6.1.3. Forecast Intensity errors (Central Pressure and Max Sustained Wind)

The mean absolute error (MAE) in the forecast of central pressure (CP)/minimum Sea level Pressure (min SLP) and maximum sustained wind (MSW) for NCUM-R and NCUM-G models is shown in Figure 25. The average error in MSW and CP is low in NCUM-G. At the initial time, the MAE in CP (MSW) is <10 hPa (10 kt) in NCUM-G. The magnitude of CP is lower in NCUM-R at the initial time as compared to NCUM-G. This is also reflected in Figure 26, where NCUM-G shows very realistic representations of MSW and CP with different ICs. However, there is some over-prediction in NCUM-R.

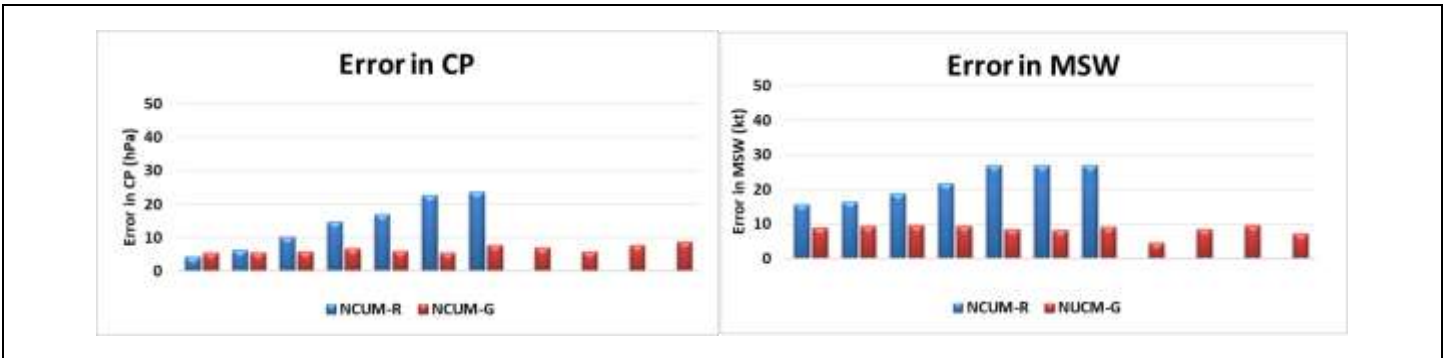


Figure 25. Mean Absolute Error (MAE) in CP (hPa) and MSW (kt) at different forecast lead times.

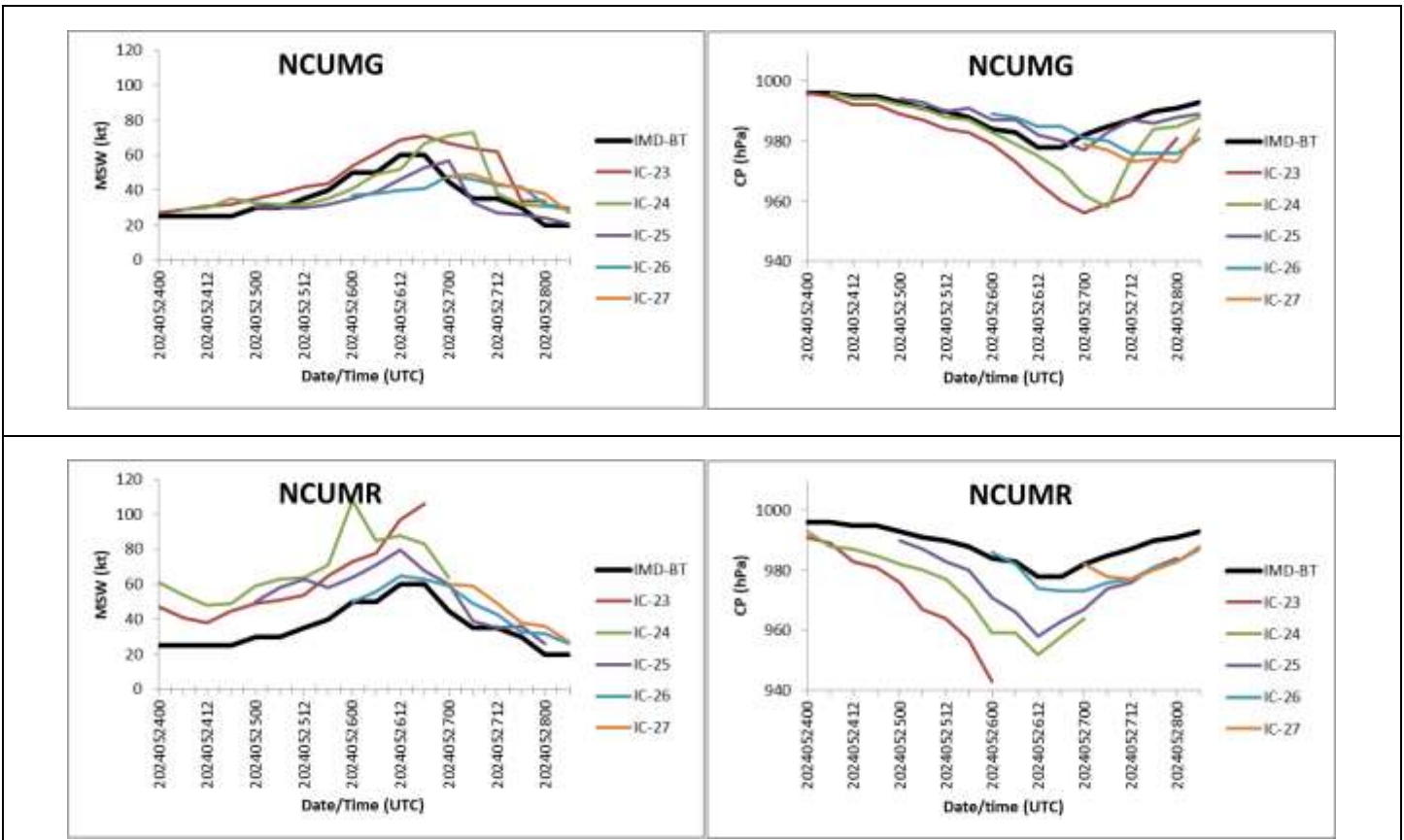


Figure 26. Intensity is given by MSW (left) & CP (right) in NCUM-G (top) and NCUM-R (bottom) forecasts with different initial conditions from 23-28th May 2024.

6.1.4. Forecast Landfall Error

As per the IMD best track data, the SCS Remal landfall time is 17-19 UTC on 28th May, and the position is 21.75^oN and 89.20^oE. The forecast landfall errors have been computed using the first forecast position on the land. NCMRWF models show the landfall over Bangladesh and adjoining coastal regions since 21st May (120 hr in advance). The forecast landfall time errors are in the range of 6 hr except on 24th May IC of NCUM-G forecast. Landfall time errors are almost zero in the NEPS-G model forecast since 24th May. Landfall position errors are more in NCUM-G, but for a few ICs, the predictions are good, even at the early stage of the system. Moreover, NCUM-G has a very accurate prediction on 26th May (00UTC), showing landfall position errors of less than 50 km, whereas NEPS-G and NCUM-R show the landfall errors of 60 and 95km, respectively.

Table 2. Error in the forecasted landfall time and position (Forecasted time – Observed time) [-ve depicts early landfall and +ve shows delay in landfall]

	NCUMG		NCUM-R		NEPS-G	
	Position	Time	Position	Time	Position	Time
2024052112	50	-6				
2024052200	210	0				
2024052212	58	3				
2024052300	86	0				
2024052312	218	3	240	-6	50	-3
2024052400	277	12	35	-6	105	0
2024052412	270	6	35	-3	130	0
2024052500	270	3	110	-6	160	0
2024052512	260	9	270	3	140	0
2024052600	20	0	95	0	60	0
2024052612	30	0	20	0	40	0

6.1.5. Verification of Strike Probability

Cyclone strike probability is the probability of locating a cyclone within 120 km of any grid point. Verification of strike probability is presented using Relative Operating Characteristics (ROC) and Reliability diagrams (attributes diagrams). It must be noted that the verification of strike probability is presented for a period from 24-28 May 2024. The Reliability diagram gives a comparison of forecast probability against the observed frequencies. A perfect match will show all points along the diagonal line. Points above the diagonal suggest underestimation (lower forecast probabilities) while points below the diagonal suggest overestimation (higher forecast probabilities).

For the case of SCS ‘Remal’, the verification of strike probability obtained from NEPS-G is carried out using the best track data. Figure 27 shows the reliability (left) and ROC (right) plots for the strike probability verification. In the Reliability diagram, the points along the diagonal indicate the best-performing model. While some points below the diagonal indicate over-estimation of cyclone strike probability. The ROC curve of NEPS-G shows that the model has skill as the curve is away from the diagonal line of no resolution. The AROC (area under the ROC) is 0.77 which is also indicative of reasonably good resolution in the model.

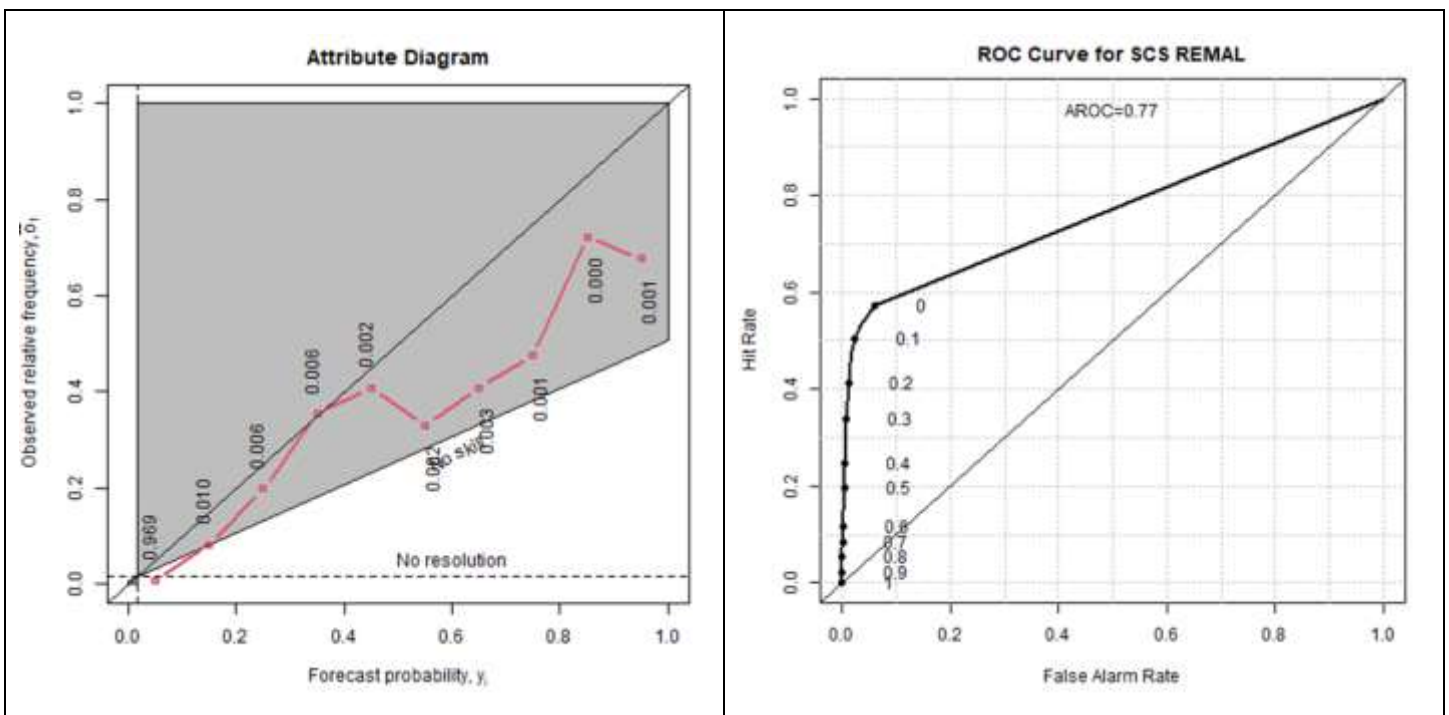


Figure 27. Verification of strike probability using reliability diagram (left) and ROC curve (right) for the case of SCS ‘Remal’.

6.1.6. CRA Verification of Rainfall Forecasts

Contiguous rain areas (CRA) verification is a spatial verification method (Ebert and Gallus 2009) that focuses on individual weather systems and verifies the properties of the forecast objects, which allows the estimation of location error of the forecast entity. A detailed description of the method with the application over India can be found for UM Rainfall forecasts over India (Ashrit et al., 2015a) and MoES Models (NCUM & GFS) in Sharma et al., (2020). Here, NCUM-G rainfall forecasts corresponding to the SCS ‘REMAL’ on the 25th and 27th May 2024 are discussed briefly using CRA verification (Figure 28a-d). The results are presented for Day-3 (*left panels*), and Day-5 (*right panels*) forecasts valid on 25th May 2024 (*top*) and 27th May 2024 (*bottom*). The CRA verification is presented for 40 mm/day threshold.

On 25th May 2024, before the landfall, the cyclone was near the coast, and observed rainfall is mainly confined to the Sea and away from the Indian coast. The Day-3 forecasts underestimate all attributes ‘grid points > 40mm’ (i.e., spatial coverage, ‘Average Rainfall’, ‘Maximum Rain’, and ‘Rain volume’). On the other hand, the Day-5 forecasts overestimate all attributes. In the Day-3 forecast, the 40mm/day object is shifted by 1.2° westwards and 0.5° southwards. In the Day-5 forecast, the object is shifted by 1.5° eastwards and 1.0° northwards. Contribution to RMSE from pattern error is dominating (77.48% in Day-3 and 72.41% in Day-5 forecasts) and next by displacement (4.09% in Day-3 and 27.12% in Day-5 forecasts).

Similarly, on 27th May 2024 (Figure 28, bottom panel), the observed rainfall (top left panels) covers parts of West Bengal and Odisha. The forecasts underestimate all the attributes in Day-3 and overestimate in Day-5. In the Day-3 forecast, the 40mm/day object is shifted by 1.5° westwards and 1.2° southwards. In the Day-5 forecast, the object is shifted by 1.5° westwards and 1.2° southwards. In this case, the contribution to RMSE is mainly from the pattern error (62.0% in Day-3 and 72.77% in Day-5) followed by displacement error (37.99% in Day-3 and 27.23% in Day-5).

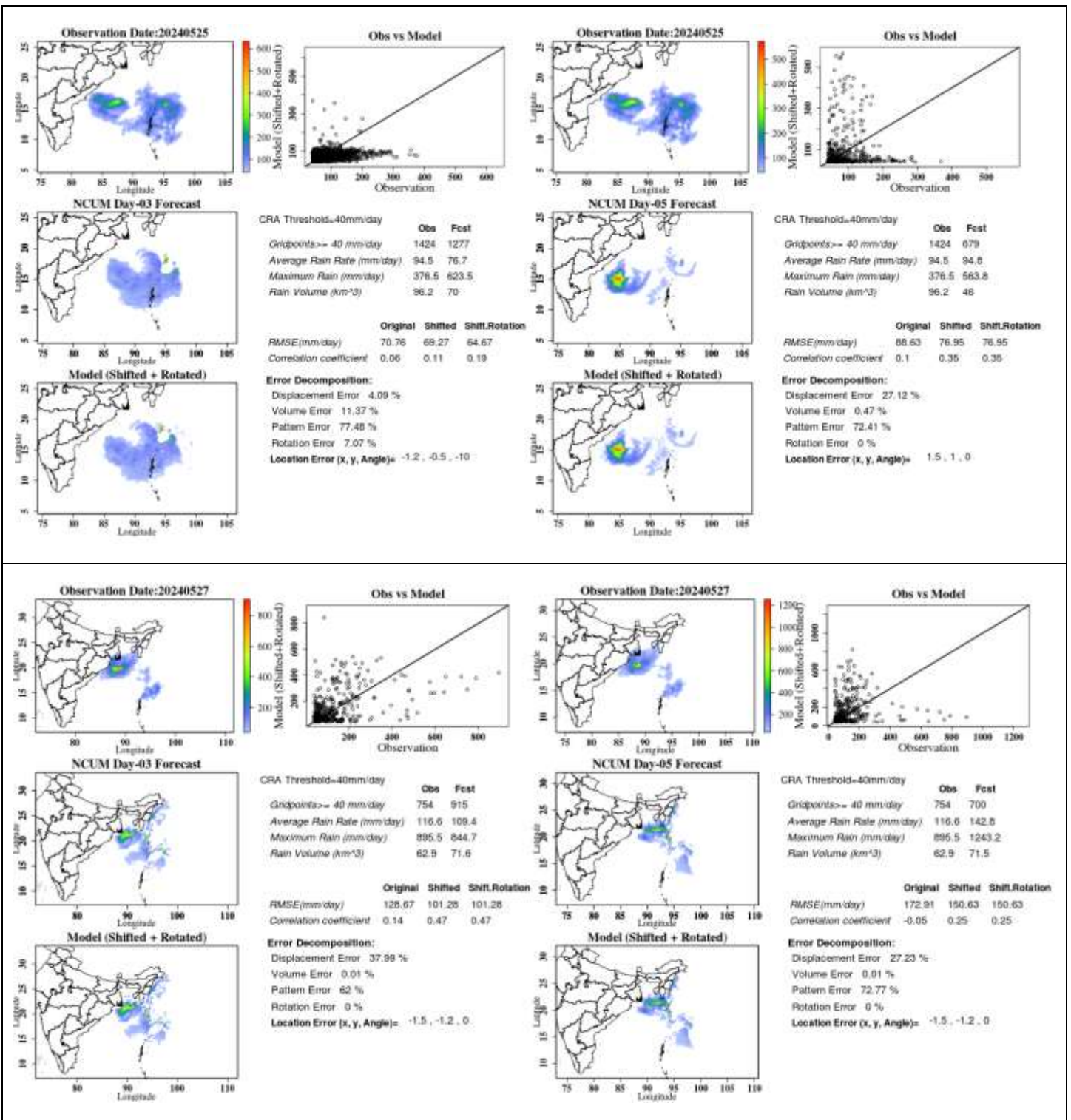


Figure 28 CRA verification of (a) Day-3 and (b) Day-5 rainfall forecasts valid on (top) 25th May 2024 and (bottom) 27th May 2024 for 40 mm/day threshold.

6.2. Western Disturbance & Heat waves

6.2.1. Western Disturbance (WD)

A WD is usually driven by the westerlies that originate in the Mediterranean region and bring rainfall to the northwestern parts of the country. Out of all the WDs as per IMD during the pre-monsoon season 2024, listed in Table 3, we have chosen a WD case for this report. Here we verify a WD that occurred during 01-03 Mar 2024. The trough in middle tropospheric westerlies can be seen in Figure 29 (top left panel) on 3rd Mar 2024, with its axis running roughly along the longitudes 68-70°E. The NCUM-G forecasts predicted this trough in Day-1 to Day-5 forecasts. The associated rainfall is primarily over Northwest and central India (Figure 30a). The NCUM-G model predicted the rainfall associated with this trough in Day-1 to Day-5 forecasts with magnitudes closer to the observation (Figure 30).

Table 3. List of MAM seasonal Western Disturbances.

S. No.	Month	Western Disturbances (WDs)	
		Total	Duration
1.	March	7	1- 3 Mar, 5-9 Mar, 9-13 Mar, 12-15 Mar, 18-21 Mar, 20-23 Mar, and 25-31Mar.
2.	April	5	1-8 Apr, 9-12 Apr, 11-17 Apr, 17-21 Apr, and 24-29 Apr.
3.	May	5	2-4 May, 4-7 May, 9-15 May, 17-22 May, and 24-27 May.

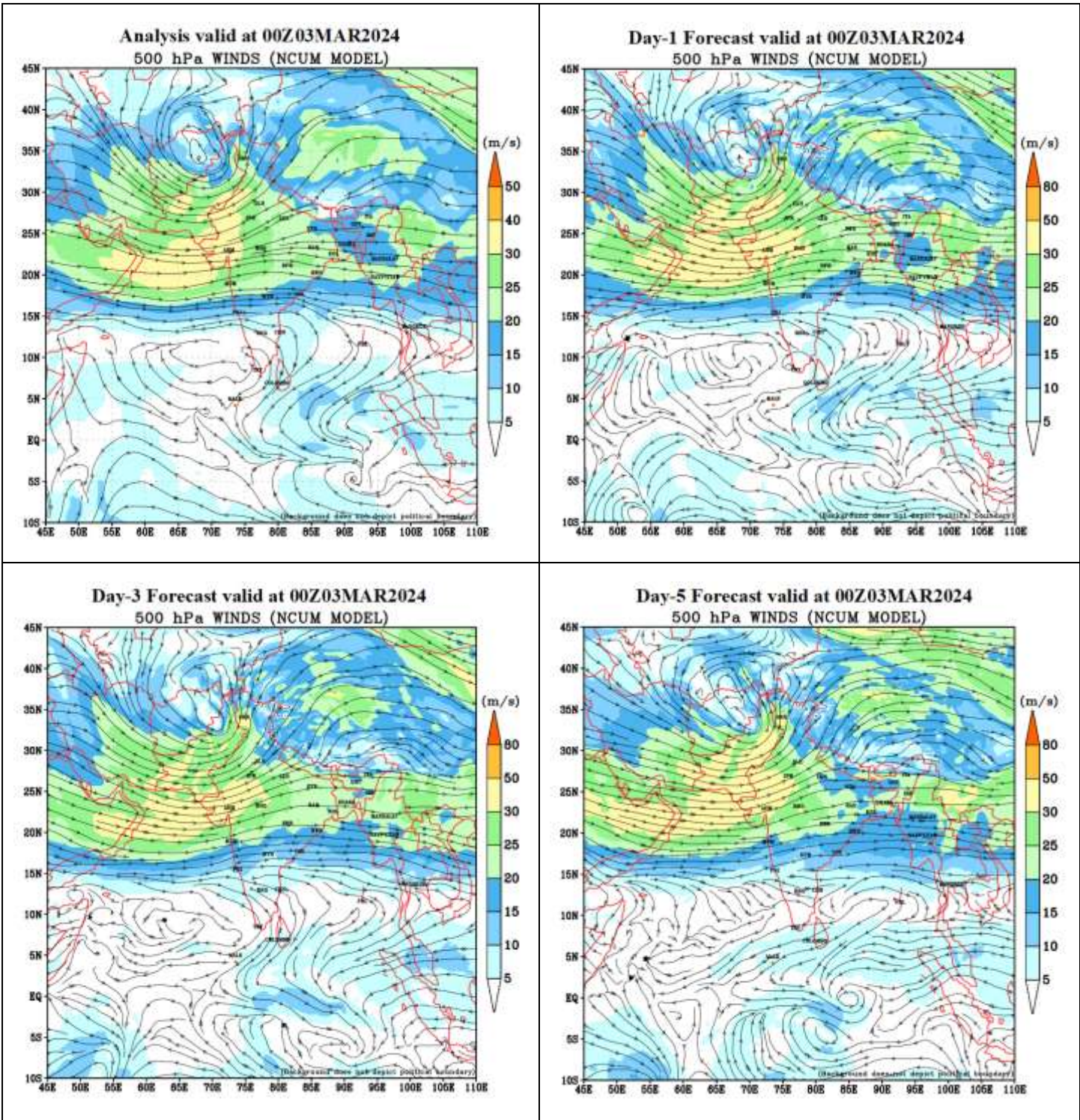
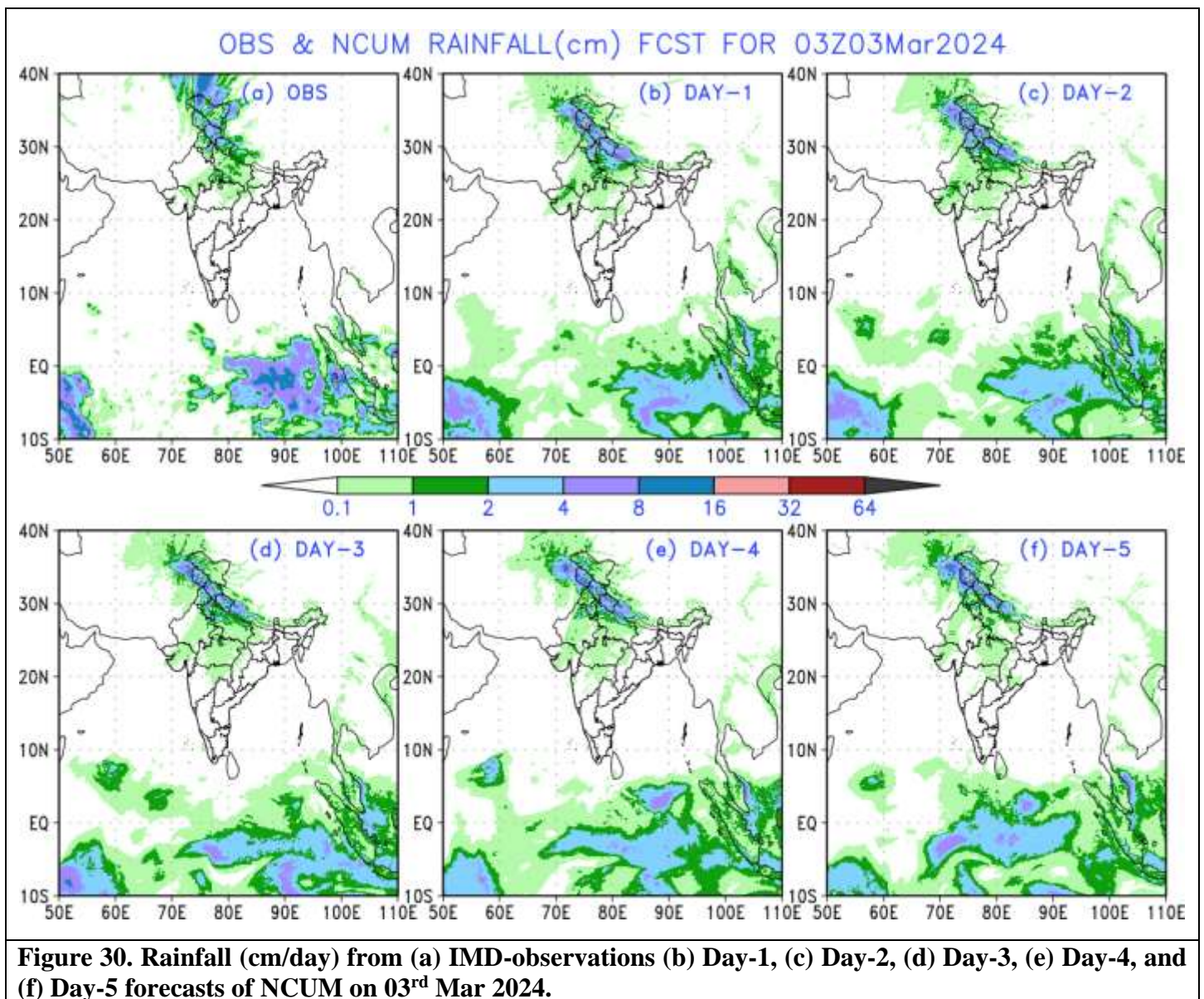


Figure 29. NCUM Winds at 500 hPa in the NCUM analysis and Day-1, Day-3, and Day-5 forecasts valid on 03Mar2024



6.2.2. Heat waves

India has experienced multiple heat wave events during MAM 2024. As per the IMD report, specifically May 2024 was the warmest. During this month, the average maximum temperature (Tmax) was above normal, with a departure from normal of 0.72°C for the country as a whole. Heatwave events, as reported by IMD during the pre-monsoon season (MAM), 2024, are listed in Table 4. Here, we verify the heat wave event that occurred over Northwest and central India from 16-31st May 2024. Figure 31 shows the temperature distribution at the end of the heatwave event on 28th May 2024, with the highest temperatures of more than 44°C is recorded over the northwestern and central parts of India. The spatial distribution of Tmax is well predicted in the NCUM-G model

forecasts till Day-5. Moreover, models have well captured the spatial distribution of maximum temperature above 44°C over Northwest and central India. However, temperature above 48°C is underestimated in Day-1 to Day-5 forecasts.

Table 4. List of MAM seasonal Heat Wave Events

S.No.	Month	Heat Wave Events
1.	March	No heat wave event
2.	April	<ul style="list-style-type: none"> ❖ Eastern India and southeast Peninsular India during 5-7 April. ❖ Odisha and West Bengal during 15-30 April. ❖ Bihar Jharkhand, Southeast Peninsular India, and interior Karnataka from 24-30.
3.	May	<ul style="list-style-type: none"> ❖ Peninsular India (mainly observed over its southeast parts covering Tamil Nadu, Interior Karnataka, and Rayalaseema) during 1-7 May ❖ Northwest and central India (mainly observed over Rajasthan, Gujarat, Madhya Pradesh, Jammu Division, Punjab, Haryana, Chandigarh, Delhi, Uttar Pradesh, Himachal Pradesh, Vidarbha, Madhya Maharashtra, and Uttar Pradesh) during 16-31 May ❖ Uttarakhand, Odisha, Chhattisgarh, and Bihar during 28-31 May.

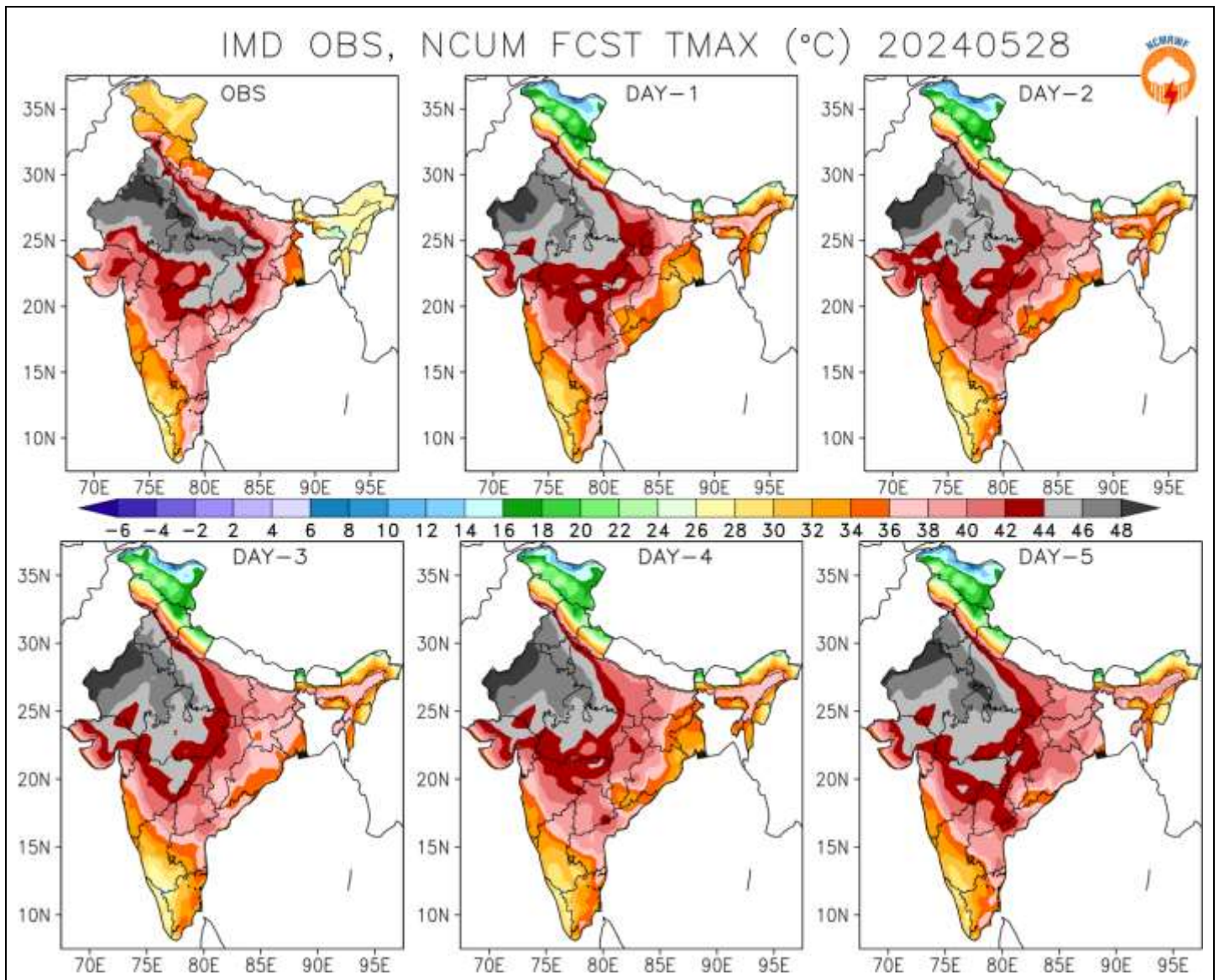


Figure 31. Spatial distribution of observed maximum temperature (top left panel) and model forecasts for different lead-times on 28th May 2024.

6.2.3. Observed and forecasted daily Tmax time series

Further, verification of the Tmax forecasts based on the NEPS ensemble is shown for several locations over Northwest India. Observed Tmax data is obtained from SYNOP stations over India via the GTS network. Figure 32 shows the forecasts with IC of 09th May 2024 for Delhi, 11th May 2024 for Amritsar, 12th May Agra, and 19th May 2024 for Bikaner. The NEPS control (red), ensemble mean (blue), and ensemble members (green) are compared with the observations (black). Observed Tmax generally lies within the spread of ensemble members. Ensemble mean shows a good match with the observations and successfully predicts a sharp rise/fall in value consistent with observations. The sharp increase in observed Tmax in Delhi and Amritsar by about $\sim 5^{\circ}\text{C}$ between

14 -19th and 14 -21st May 2024, respectively, is accurately predicted. Similarly, for IC of 12th (19th May 2024), the heatwave event over Agra (Bikaner) during 13-18th (25-28th) May 2024 is also well captured.

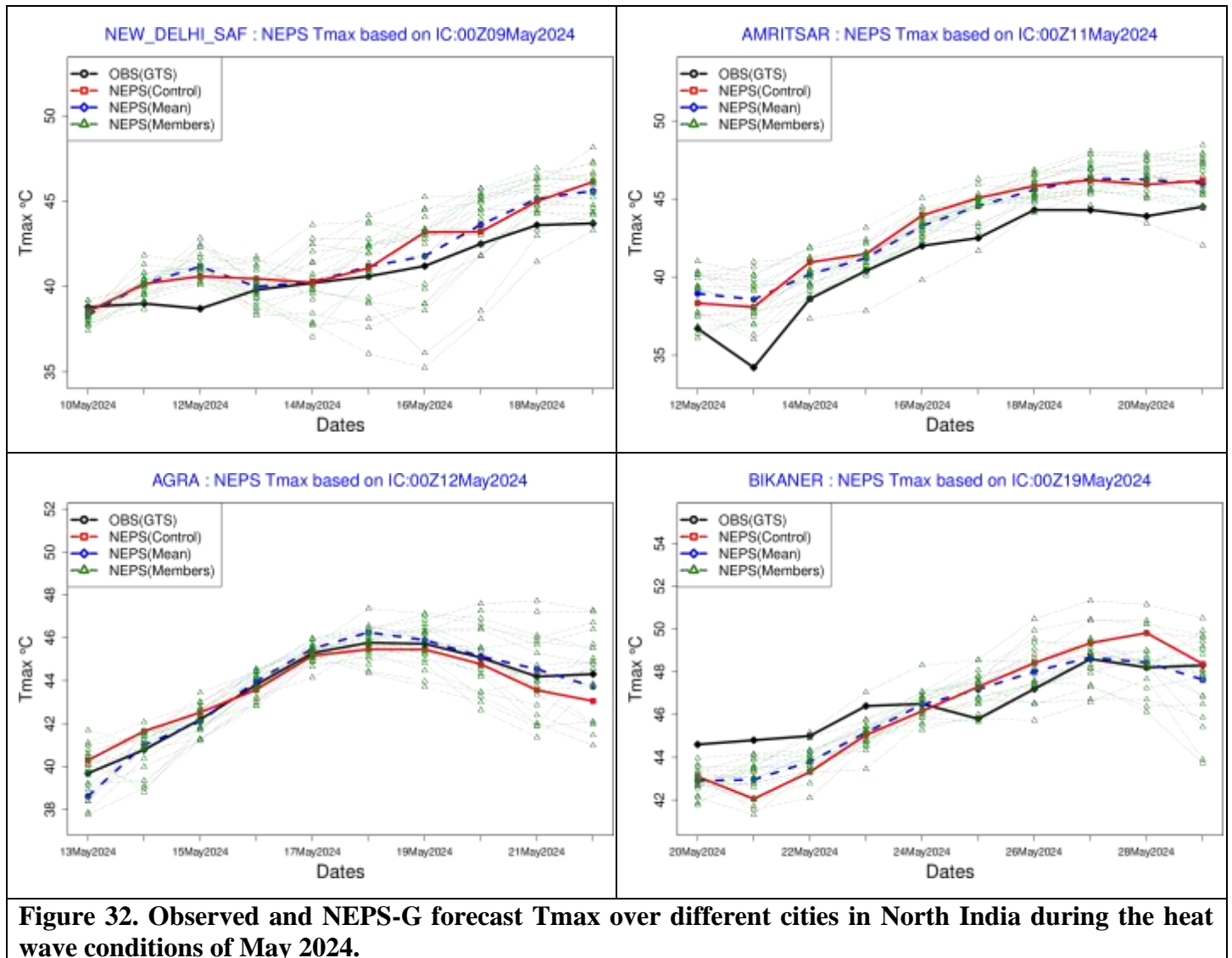


Figure 32. Observed and NEPS-G forecast Tmax over different cities in North India during the heat wave conditions of May 2024.

7. Summary

This report documents the performance of the NCMRWF model forecasts during the Pre-monsoon season MAM 2024. The verification results are presented to address both forecasters and model developers. The information on biases in the forecast winds, temperature, humidity, rainfall, etc., is crucial for the forecasters to interpret the model guidance for forecasting. Additionally, information on recent improvements in the model skill adds to confidence in the model forecasts. The results of the study can be summarized below.

7.1. NCUM-G Mean analysis and anomalies during MAM 2024

- ❖ *The low-level winds at 850 hPa and 700hPa represent northwesterly winds with increasing altitudes having strength ranging from 5 to 10 m/s and the presence of anticyclone over the southern peninsular region. Further, with increasing altitude, mean winds in the north Indian region enhanced from ~18m/s at 500 hPa to more than 40m/s in the upper troposphere.*
- ❖ *The anomalous winds at 850hPa and 700hPa indicate contrasting features in the north and south with weaker and stronger winds in NCUM-G analysis with respect to ERA5 reanalysis, respectively, over the Indian subcontinent. At 850 hPa level, an anomalous cyclonic circulation is present over northwestern India. This circulation is becoming enhanced at 700 hPa level w.r.t ERA5. On the other hand, over the equatorial Indian Ocean, specifically in southern latitudes, the winds are weaker in NCUM-G analysis resulting in strong anomalous easterlies. Overall, in north India, the magnitude of winds is relatively lower compared to ERA5 reanalysis due to persistent anomalous easterlies.*
- ❖ *Low level (850 and 700 hPa) temperature anomalies indicate that the Pre-monsoon 2024 is warmer than the climatology, with magnitudes between more than 1° ~ 2°C over the Indian land region, excluding some parts of the north-western Indian region. The warmer temperatures stretch from northwest to southeast India, covering the Indo-Gangetic plains. The temperature anomalies across India still indicate warmer than the climatology at both 500 and 200 hPa levels.*
- ❖ *MAM 2024 indicates a higher percentage of RH compared to the climatology across India, excluding the IGPs. Over the oceans surrounding the Indian subcontinent, positive anomalies are observed over the western oceanic region, including the AS, while negative anomalies are present over the eastern oceanic region, including the BoB at 850 hPa. At 700 and 500 hPa, positive anomalies are noted over the oceanic regions, except for the southern BoB.*

7.2. NCUM-G Systematic Errors

- ❖ *Systematic errors in winds at 850 hPa from Day-1 forecasts show a westerly wind bias over the northern Indian region and along the west coast. Enhanced north westerlies are more prominent along the west coast. With forecast lead times, these errors in low-level winds enhance, and this could be due to the enhanced convective activity around the equatorial regions during the Pre-monsoon season. Similar systematic errors in winds are also noticed at 700 hPa level over the Indian region. In addition, westerly wind bias is more prominent at 700 hPa level over the western equatorial Indian Ocean in Day-3 and Day-5 forecasts. Systematic errors at 200 hPa level winds show enhanced divergent circulation centered around central India as seen in Day-3 forecasts, and this divergent circulation shifted westward in Day-5 forecasts with enhanced error magnitudes.*

- ❖ *The model shows warm bias ($\sim 0.5-1^\circ\text{C}$) occupied over most of the Indian land mass, and the magnitude of this bias is increasing with forecast lead time. These error increments at 850hPa temperatures are also more prominent over IGP regions. On a similar note, temperature errors at 700 hPa also show warm bias ($>1^\circ\text{C}$) over most of the Indian land region. Interesting, to see that the bias over the south BoB region reverse sign and now exhibits cold bias compared to the 850hPa level. At 500 hPa (200 hPa) level, temperature exhibits warm (cold) bias over the Indian land region, including surrounding oceanic regions, and the magnitude of the bias is increasing in forecasts with lead time.*
- ❖ *Systematic errors show a large dry bias over Indian land regions at 850hPa level, and the dryness is enhancing with forecast lead time. The presence of low-level anticyclones over the Indian sub-continent induces enhanced warming, which could be one primary reason for the negative RH values over the central Indian region. On the contrary, oceanic regions exhibit moist bias, as evidenced by positive RH values, except for the South China Sea, head BoB, and some parts of AS. Interestingly the moist bias observed over the oceanic regions (i.e., AS and BoB) at 850 hPa level change sign to negative, and dry bias is seen at 700 hPa level. Additionally, the moist bias south of the equator is getting intensified in the Day-3 and Day-5 forecast and the entire column is occupied with excess moisture at 700 hPa levels.*
- ❖ *Seasonal mean winds at 10m level from the analysis show the presence of relatively strong north westerlies over the Arabian Sea (AS), south-westerlies over head BoB, and weak westerlies over the tropical Indian Ocean (TIO), while below TIO strong easterlies around 80°E . The systematic error in the forecasts depicts few notable features. (i) The north-westerly wind bias along the west coast over northern AS and south-westerly wind bias along the east coast over BoB on Day 1 forecast is enhancing its strength with forecast lead time. (ii) On a similar note, the easterly wind bias seen in the Day-1 forecast around the equator and south of the equator close to the maritime continent, and its direction changes to westerly wind biases in the Day-5 forecast.*
- ❖ *Systematic errors show a relatively warm bias over the Indian land regions and north of 40°N latitude regions. Interestingly these warm biases are increasing with forecast lead time, especially over the Indian region. This can be attributed to the dry north-westerly winds from the northwest entering Indian land and north AS. In addition, most of the oceanic regions of BoB and AS exhibited cold bias of the range $<-0.5^\circ\text{C}$ in all the forecast times.*
- ❖ *Seasonal mean PWAT shows a large value ($> 60\text{mm}$) around the equatorial regions, especially over the Maritime continent (MC), owing to the presence of warm pools and associated convection during pre-monsoon season over these regions. On the contrary, most of the northern and central Indian regions are dry with very less PWAT values (5-15mm). However, extreme southeast peninsular India exhibits moderate PWAT values around 35-40 mm due to the westerly winds from the MC region. Systematic error in PWAT shows a column dry over Indian land regions on Day 1, this dryness in the column is enhancing with forecast lead time, and its magnitudes are maximum on Day 5. In addition, positive bias in PWAT is seen over the south of equatorial regions.*

7.3. Forecast Verification

- ❖ *Much of the Indian subcontinent is dry except for the northern parts of India, the southern peninsula, the eastern coastal region, and the northeastern regions. NCUM-G model forecasts overestimate the rainfall, particularly over Kerala, along the eastern coastal and the northeastern regions, while underestimating over the oceanic regions.*
- ❖ *For different rainfall thresholds (3-30mm/day) POD (FAR) shows a decrease (increase) in value, respectively. $POD \geq 0.3$ for rainfall up to 6 mm/day. The BIAS score (frequency bias) indicates that forecasts overestimate the frequency of all thresholds. The values of PSS and SEDI up to 3-5 mm/day indicate reasonable skill.*
- ❖ *The categorical scores for Tmax are also computed for MAM 2024. The POD indicates a slight increase with the thresholds from 30 °C to 44 °C, while the PSS score is nearly constant and below 0.3 till 40 °C; thereafter, it slightly increases to above 0.3. FAR scores all over India as a whole show relatively large values >0.6 up in all temperature thresholds and varies between 0.6-0.8 in all forecast lead times.*

7.4. Verification for Significant Weather

Bay of Bengal SCS 'REMAL' during 24-28 May 2024, Western Disturbances, and Heat waves formed significant weather events of MAM 2024.

- ❖ ***Initial Position Error:** Mean initial position errors are lower in NEPS-G (46 km).*
- ❖ ***Direct Position Error:** NEPS-G shows track errors less than 100 km up to 36 hr. The initial error is comparable (64 and 63 km) in both NCUM-G and NCUM-R models.*
- ❖ ***Landfall Position & Time error:** The landfall position errors <50 km are seen from NCUM-R on 26th May forecasts (00Z). In general Landfall time errors in the models are in the range of 6 hr where NCUM-R shows faster movement. The best forecast in terms of landfall time is seen in NEPS-G.*
- ❖ ***Intensity verification (NCUM-G & NCUM-R):** MAE in both CP and MSW is lower in NCUM-G.*
- ❖ ***Verification of strike probability (NEPS-G & NEPS-R):** ROC and Reliability diagrams are used for this purpose. The NEPS-G model is over-forecasting. The ROC curves show that the models have reasonable skill (ROC is 0.77).*
- ❖ *We have also verified a WD that occurred during 01-03rd May 2024. The NCUM-G forecasts predicted this trough on Day-1 to until Day-5 forecasts. This western disturbance brought rainfall primarily over Northwest and Central India. The NCUM-G model predicted the rainfalls associated with this trough in Day-1 to Day-5 forecasts with magnitudes closer to the observations.*
- ❖ *Further, during MAM 2024 heatwave conditions are verified from model forecasts against observations for different forecast lead times. Overall, the heat wave conditions are predicted very well 3 days earlier, and after that model skill is reduced.*

References

1. Ashrit, R., Elizabeth Ebert, Ashis K. Mitra, Kuldeep Sharma, Gopal Iyengar and E.N. Rajagopal 2015a: Verification of Met Office Unified Model (UM) quantitative precipitation forecasts during the Indian Monsoon using the Contiguous Rain Area (CRA) method. NMRF/RR/03/2015
2. Ashrit R, Sharma K, Dube A, Iyengar G R, Mitra A K and Rajagopal E N 2015b: Verification of short-range forecasts of extreme rainfall during monsoon; *Mausam* 66 375–386, 607.
3. Barker, D., 2011. Data assimilation-progress and plans, MOSAC-16, 9-11 November 2011, Paper16.6.
4. Ebert, E.E. and W.A. Gallus, 2009: Toward better understanding of the contiguous rain area (CRA) method for spatial forecast verification. *Wea. Forecasting*, 24, 1401-1415.
5. Hersbach H, Bell B, Berrisford P, et al. 2020: The ERA5 global reanalysis. *Q J R Meteorol Soc.* 2020;146:1999–2049. <https://doi.org/10.1002/qj.3803>
6. Jolliffe, I. T., and D. Stephenson, 2012: *Forecast Verification: A Practitioner's Guide in Atmospheric Science*, John Wiley & Sons, Ltd.
7. Kumar Sumit, A. Jayakumar, M. T. Bushair, Buddhi Prakash J., Gibies George, Abhishek Lodh, S. Indira Rani, Saji Mohandas, John P. George and E. N. Rajagopal 2018: Implementation of New High Resolution NCUM Analysis-Forecast System in Mihir HPCS. NMRF/TR/01/2019, 17p.
8. Kumar Sumit, M. T. Bushair, Buddhi Prakash J., Abhishek Lodh, Priti Sharma, Gibies George, S. Indira Rani, John P. George, A. Jayakumar, Saji Mohandas, Sushant Kumar, Kuldeep Sharma, S. Karunasagar, and E. N. Rajagopal 2020: NCUM Global NWP System: Version 6 (NCUM-G:V6), NMRF/TR/06/2020.
9. Kumar Sumit, Gibies George, Buddhi Prakash J., M. T. Bushair, S. Indira Rani and John P. George 2021: NCUM Global DA System: Highlights of the 2021 upgrade, NMRF/TR/05/2021.
10. Mitra, A. K., A. K. Bohra, M. N. Rajeevan and T. N. Krishnamurti, 2009: Daily Indian precipitation analyses formed from a merged of rain-gauge with TRMM TMPA satellite derived rainfall estimates, *J. of Met. Soc. of Japan*, 87A, 265-279.
11. Mitra, A. K., I. M. Momin, E. N. Rajagopal, S. Basu, M. N. Rajeevan and T. N. Krishnamurti, 2013, Gridded Daily Indian Monsoon Rainfall for 14 Seasons: Merged TRMM and IMD Gauge Analyzed Values, *J. of Earth System Science*, 122(5), 1173-1182.
12. Sharma K., S. Karunasagar and Raghavendra Ashrit 2020: CRA Verification of GFS and NCUM Rainfall Forecasts for Depression cases during JJAS 2018. /NMRF/RR/05/2020
13. Sharma, K., Ashrit, R., Kumar, S. et al. Unified model rainfall forecasts over India during 2007–2018: Evaluating extreme rains over hilly regions. *J Earth Syst Sci* 130, 82 (2021). <https://doi.org/10.1007/s12040-021-01595-1>
14. Srivastava A K, Rajeevan M and Kshirsagar S R 2009: Development of a high resolution daily gridded temperature data set (1969–2005) for the Indian region; *Atmos. Sci. Lett.* 10 249–254, <https://doi.org/10.1002/asl.232>
15. Stephenson D.B., B. Casati, C.A.T. Ferro and C.A. Wilson, 2008: The extreme dependency score: a non-vanishing measure for forecasts of rare events. *Meteorol. Appl.*, 15, 41-50.
16. Walters, D., and co-authors: The Met Office Unified Model Global Atmosphere 6.0/6.1 and JULES Global Land 6.0/6.1 configurations, *Geosci. Model Dev.*, 10, 1487–1520, <https://doi.org/10.5194/gmd-10-1487-2017>, 2017.
17. Wilks D S 2011 (eds) *Statistical methods in the atmospheric 807 sciences*; 3rd edn, Elsevier, 676p